

Supporting Information

Lipid Nanoparticle Delivery of Small Proteins for Potent In Vivo RAS Inhibition

Rebecca M. Haley^{1†}, Alexander Chan^{1†}, Margaret M. Billingsley¹, Ningqiang Gong¹, Marshall S. Padilla¹, Emily H. Kim², Hejia Wang³, Dingzi Yin⁴, Kirk J. Wangensteen^{4}, Andrew Tsourkas^{1*}, Michael J. Mitchell^{1*}*

¹Department of Bioengineering, University of Pennsylvania, Philadelphia, PA 19104, United States

²Department of Chemical and Biomolecular Engineering, University of Pennsylvania, Philadelphia, PA 19104, United States

³Department of Biochemistry and Molecular Biophysics, University of Pennsylvania, Philadelphia, PA 19104, United States

⁴Division of Gastroenterology and Hepatology, Department of Medicine, Mayo Clinic, Rochester, MN 55902, United States

†Contributed equally to this work, *Corresponding Author

E-mails: wangenstein.kirk@mayo.edu, atsourk@seas.upenn.edu, mjmitch@seas.upenn.edu

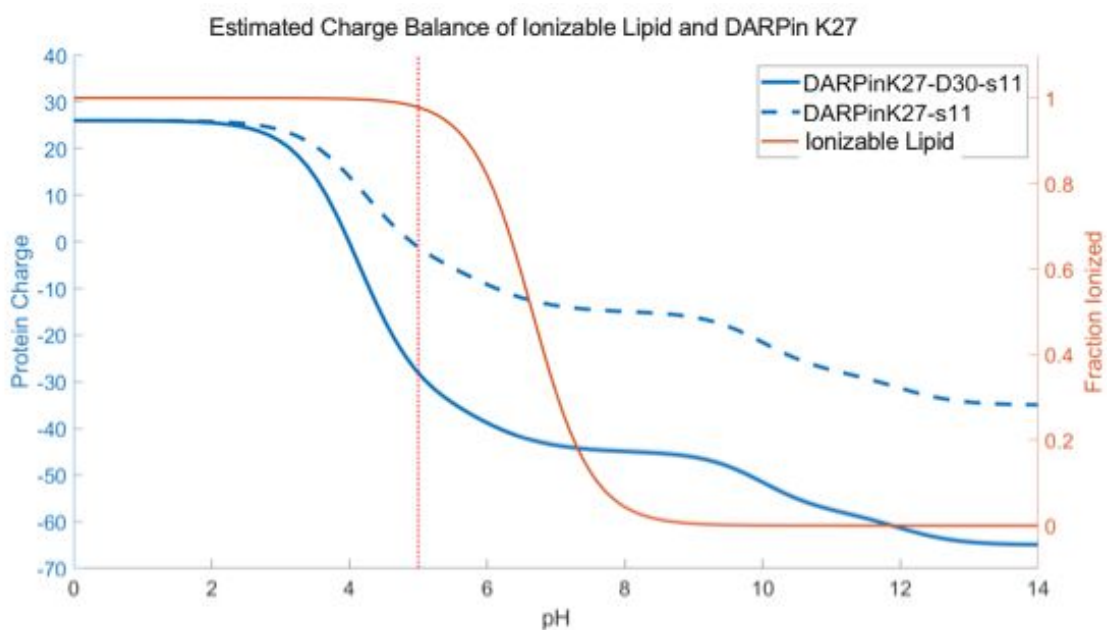


Figure S1. Estimated charges of ionizable lipid and K27 at variable pH, to illustrate the need for formulation at a pH which optimizes charge on both components. At pH 5, used in the optimized LNP formulations herein, the ionizable lipid remains positively charged and the DARPin remains negatively charged.

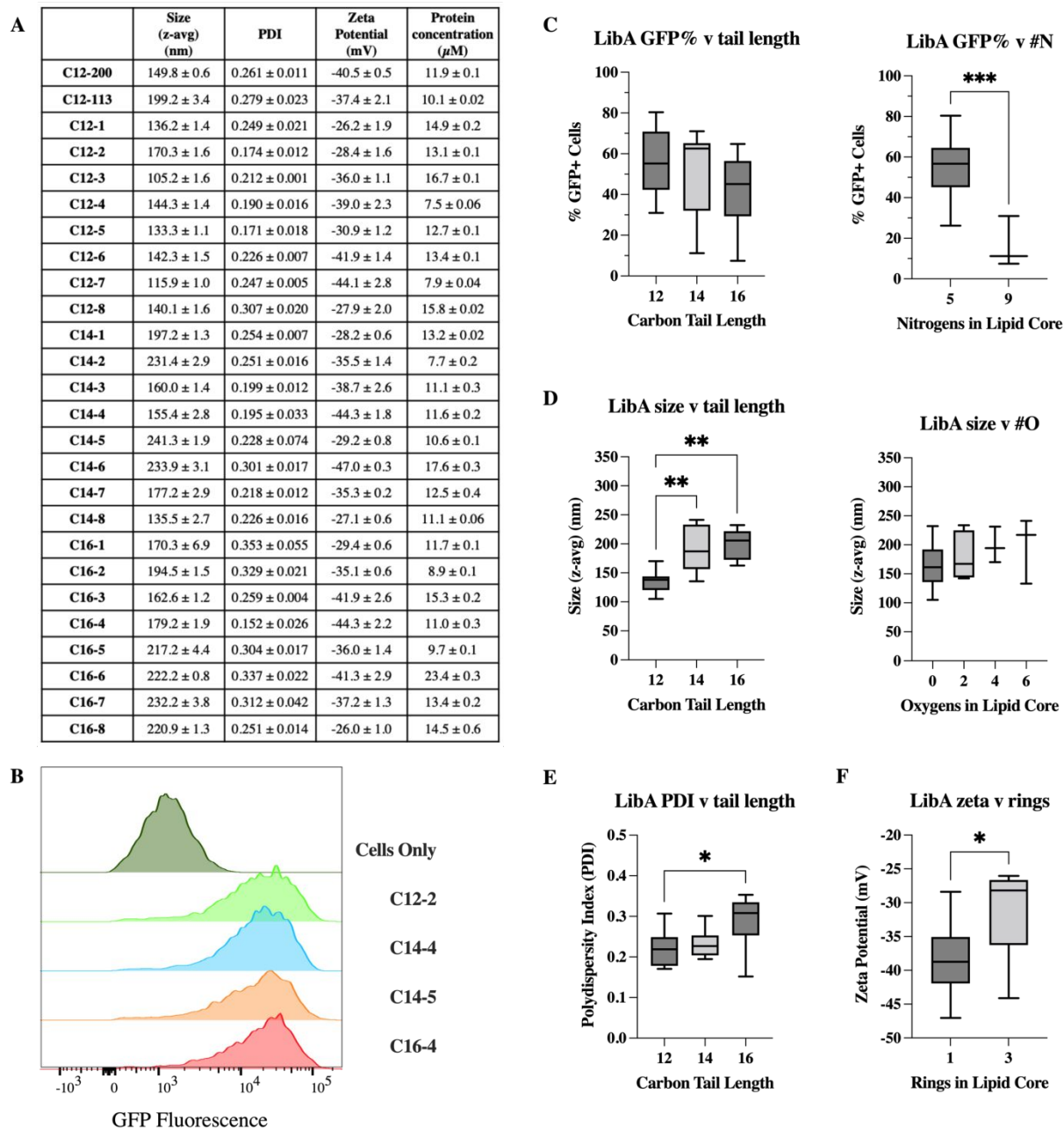


Figure S2. Additional characterization and analysis of LNPs formulated in library A. (A) Size (z-avg), PDI, surface zeta potential, and protein concentration of LNPs in library A. (B) Representative flow plots of untreated (control) and top performing LNPs from library A (C12-2, C14-4, C14-5, and C16-4). (C) Parameters—carbon tail length and number of Nitrogens in the polyamine core—with significant influence on delivery efficiency, measured by %GFP+ cells. (D) Parameters—carbon tail length and number of Oxygens in the polyamine core—with

significant influence on size (z-avg). (E) PDI was influenced by carbon tail length. (F) Surface zeta potential, was influenced by the number of rings in the lipid core.

Identifier	Ionizable Lipid	Helper (Neutral) Lipid	DOTAP%	Protein:Lipid Molar Ratio	Size (z-avg) (nm)	PDI	Zeta Potential (mV)	Protein Concentration (μ M)
C12-200	C12-200	DSPC	50	1:50	253.2 \pm 4.5	0.363 \pm 0.019	-29.7 \pm 0.5	10.5 \pm 0.3
B1	C12-2	DSPC	30	1:30	206.4 \pm 34.8	0.251 \pm 0.109	-31.2 \pm 0.4	17.0 \pm 0.1
B2	C12-2	DOPE	40	1:50	221.6 \pm 1.3	0.204 \pm 0.017	-28.1 \pm 0.8	11.2 \pm 0.5
B3	C12-2	DSPC	50	1:80	192.0 \pm 2.1	0.209 \pm 0.020	-25.5 \pm 1.0	5.6 \pm 0.05
B4	C12-2	DOPC	60	1:120	178.1 \pm 2.6	0.128 \pm 0.033	8.2 \pm 0.5	3.2 \pm 0.09
B5	C14-4	DSPC	40	1:80	174.8 \pm 2.6	0.137 \pm 0.034	14.1 \pm 2.5	2.4 \pm 0.07
B6	C14-4	DOPE	30	1:120	198.4 \pm 4.4	0.237 \pm 0.016	9.5 \pm 1.2	2.2 \pm 0.04
B7	C14-4	DSPC	60	1:30	161.9 \pm 2.8	0.221 \pm 0.011	-37.3 \pm 1.1	12.8 \pm 0.4
B8	C14-4	DOPC	50	1:50	214.8 \pm 2.1	0.298 \pm 0.055	-29.7 \pm 0.8	9.5 \pm 0.2
B9	C14-5	DSPC	50	1:120	208.0 \pm 1.5	0.261 \pm 0.007	11.1 \pm 2.6	5.8 \pm 0.1
B10	C14-5	DOPE	60	1:80	180.1 \pm 1.0	0.108 \pm 0.003	13.7 \pm 0.4	2.7 \pm 0.1
B11	C14-5	DSPC	30	1:50	251.3 \pm 5.2	0.368 \pm 0.055	-28.6 \pm 0.2	11.3 \pm 0.1
B12	C14-5	DOPC	40	1:30	240.6 \pm 4.1	0.323 \pm 0.075	-32.5 \pm 1.2	10.9 \pm 0.4
B13	C16-4	DSPC	60	1:50	172.2 \pm 1.1	0.182 \pm 0.019	-37.5 \pm 2.0	10.4 \pm 0.2
B14	C16-4	DOPE	50	1:30	185.1 \pm 2.3	0.304 \pm 0.029	-31.5 \pm 1.1	15.4 \pm 0.2
B15	C16-4	DSPC	40	1:120	189.2 \pm 1.3	0.106 \pm 0.001	-20.7 \pm 1.3	5.5 \pm 0.5
B16	C16-4	DOPC	30	1:80	281.3 \pm 6.9	0.287 \pm 0.020	-34.1 \pm 1.4	5.7 \pm 0.2

Figure S3. Formulation parameters and additional characterization of LNPs formulated in library B, including size, PDI, zeta potential, and protein concentration.

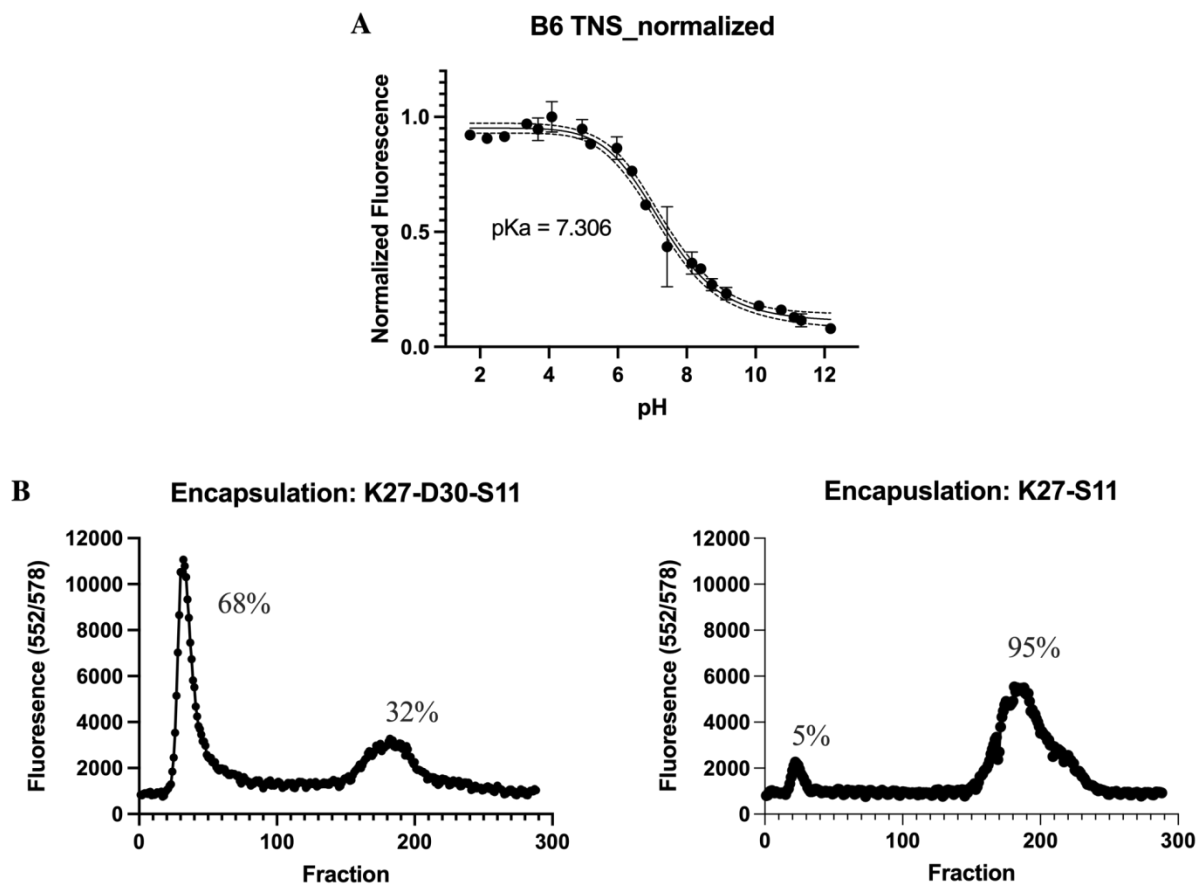


Figure S4. Additional characterization of the top performing LNP (B6). **(A)** TNS of B6 to evaluate ionizability of the LNP. pKa was found to be 7.306. **(B)** Encapsulation efficiency of B6 was evaluated using TAMRA-labelled K27 and a size exclusion gravity column. 68% of negative charged modified K27 (left) was found in fractions containing LNPs. In contrast, only 5% of non-charge modified K27 (right) was found in fractions containing LNPs.

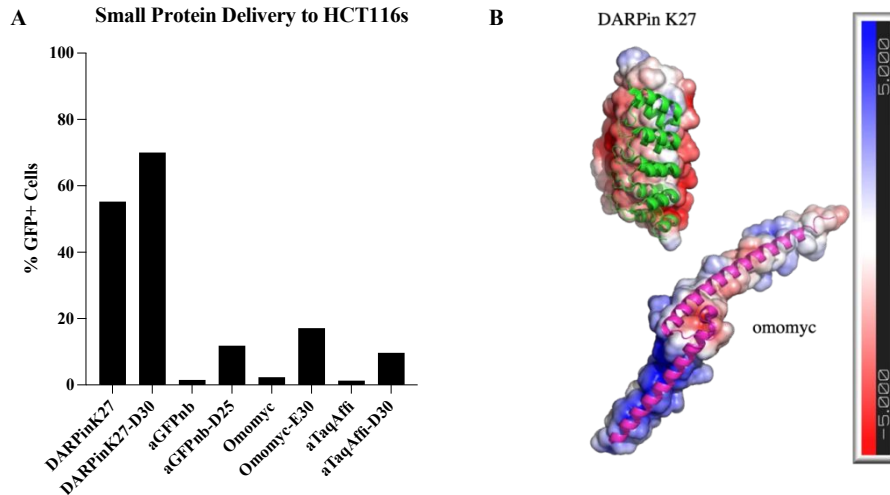


Figure S5. Alternative small proteins encapsulated and delivered to HCT116 cells *in vitro* using B6 LNPs. **(A)** Among the small proteins tested—nanobodies, omomyc, and affibodies—charge modification improved delivery, but no other small proteins were found to have good delivery with the K27-optimized B6 formulation. **(B)** Differences in structure and local charge between small protein scaffold types likely cause different requirements for LNP delivery system. PDB IDs 5O2S and 5I50 for DARPin K27 and omomyc, respectively.

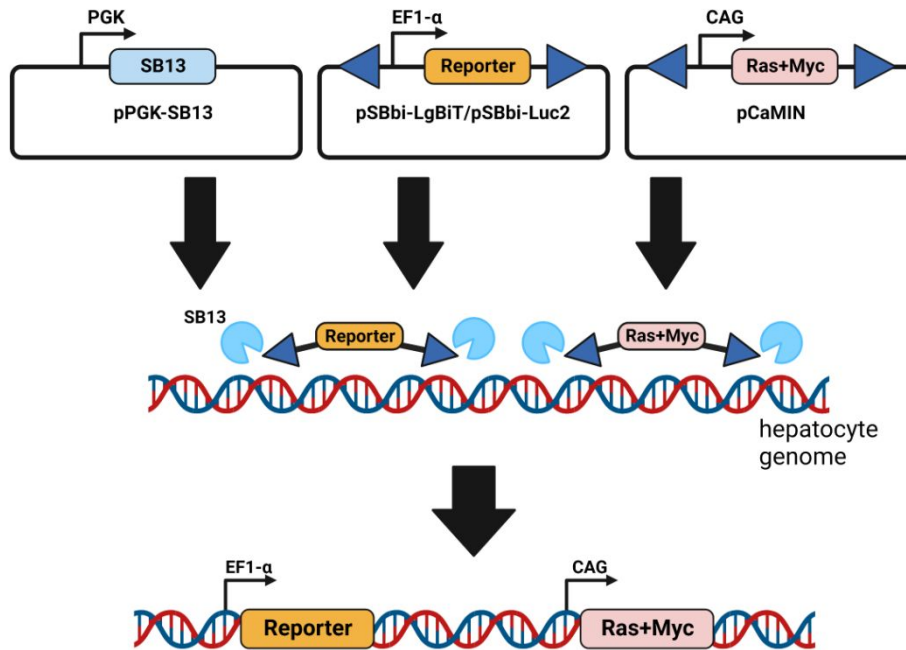


Figure S6. *Sleeping Beauty* transposon system used to insert different plasmids for different parts of this work: pPGK-SB13 for SB13 transposase plasmid, pSBbi-LgBiT or pSBbi-

Luc2 for split NanoLuc and firefly Luciferase reporters, and pCaMIN for the oncogenes MYC and NRAS^{G12V}, which induce tumor growth. Figure was created with Biorender.com.

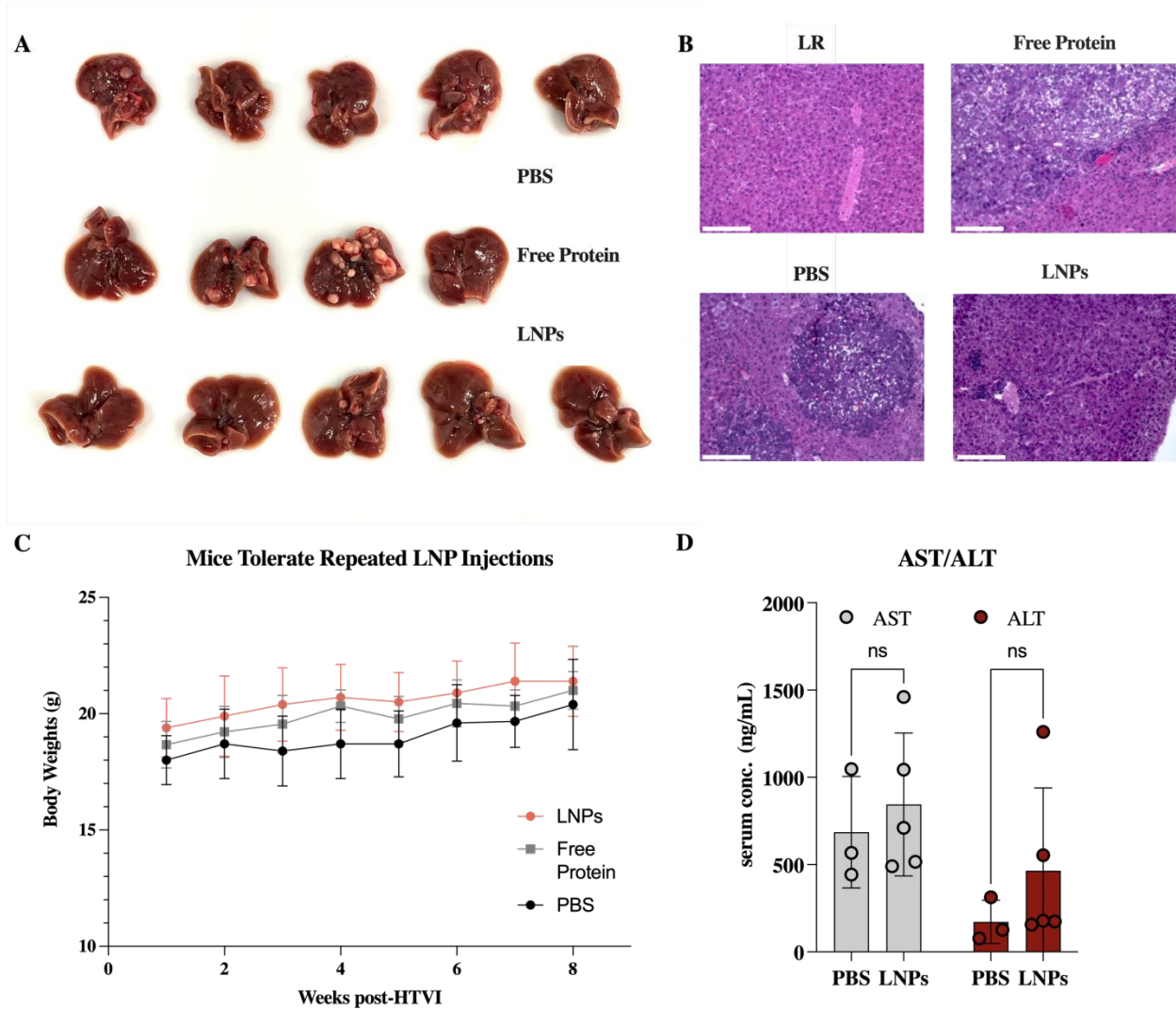


Figure S7. Additional *in vivo* therapeutic data. **(A)** Liver images from a subset of mice used in this study, showing type of tumor produced by HTVI method used herein. **(B)** Higher zoom on histology images (H&E stained) from Figure 9, which show tumor levels in LR (healthy), PBS, free protein, and LNP groups. Scale bar = 150 μ m. **(C)** Whole body weights of mice in this study show slight increase—due to growth—over time, with no significant difference between groups, indicating that mice tolerated repeat injections. **(D)** Serum concentrations of AST (aspartate aminotransferase) and ALT (alanine transaminase) in mice 24h after receiving PBS or LNP-

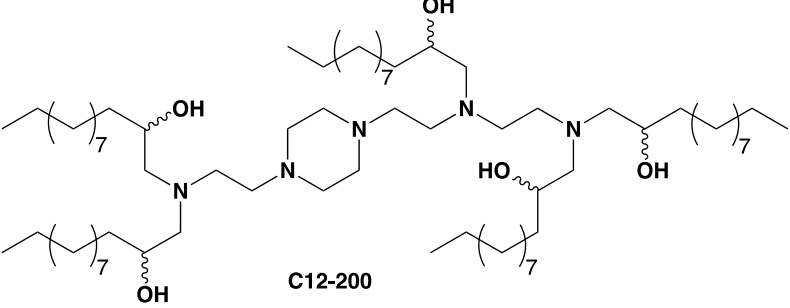
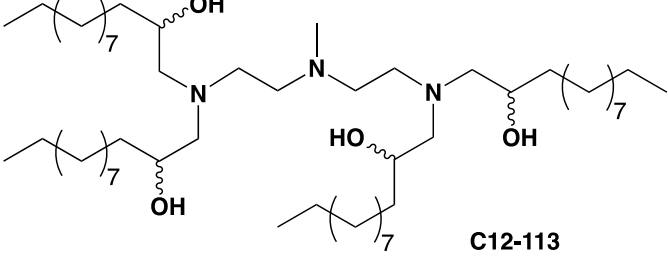
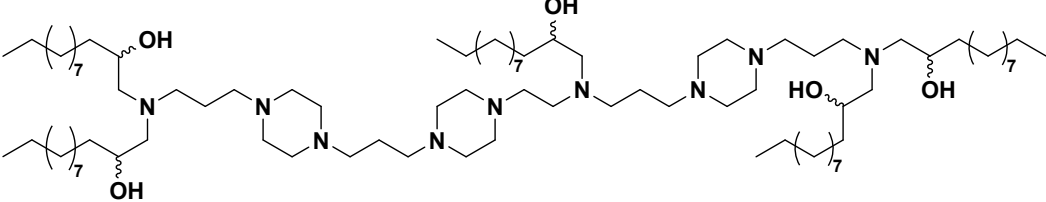
encapsulated K27-D30 at 4.5 mg/kg. Both liver toxicity markers are increased on average after LNP injection but are not statistically different from the PBS control.

Table S1. Amino acid sequences of proteins used in this work. Sequences assume elution with GGG peptide during protein purification. Underlined is the negative charge (ApP, D30 repeat sequence). In green is GFP s11, in yellow is HiBiT. Isoelectric point calculated by ExPASy pI/MW computational application.⁴⁸

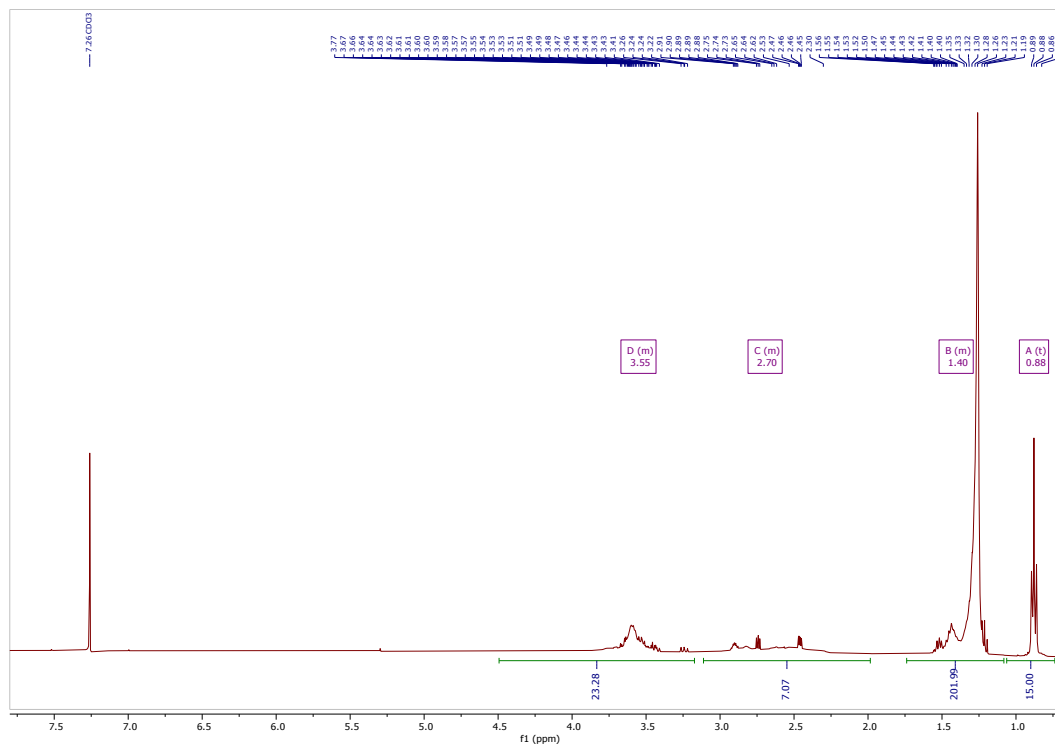
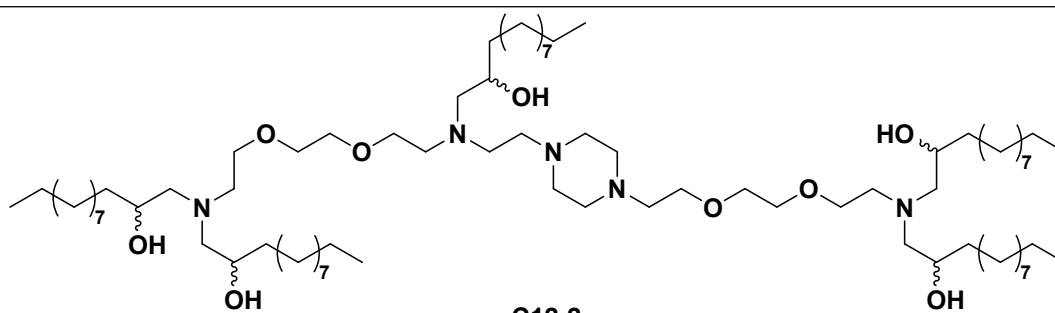
Protein Name	Amino Acid Sequence	M.W. (kDa)	Calculated Isoelectric Point
DARPinK27-S11	MDLGKKLLEAARAGQDDEVRLMANGADVNAHDTFGFTP LHLAALYGHLEIVEVLLKNGADVNADDSYGRTPHLAAMR GHLEIVEVLLKYGADVNAADEEGRTPLHLAAKRGHLEIVEV LLKNGADVNAQDKFGKTAFDISIDNGNEDLAEILQKLgsgsgg gsgsgsgsgsgsgg <u>RDHMLHEYVNAAGIT</u> sgsggsLPETGGG	21.15	4.90
DARPinK27-D30-S11	MDLGKKLLEAARAGQDDEVRLMANGADVNAHDTFGFTP LHLAALYGHLEIVEVLLKNGADVNADDSYGRTPHLAAMR GHLEIVEVLLKYGADVNAADEEGRTPLHLAAKRGHLEIVEV LLKNGADVNAQDKFGKTAFDISIDNGNEDLAEILQKLgsgsgg gss <u>RDHMLHEYVNAAGIT</u> sgsggsLPETGGG	24.49	3.99
DARPinK27n3-D30-S11	MDLGKKLLEAARAGQDDEVRLMANGADVNAHDTFGFTP LHLAALYGHLEIVEVLLKNGADVNADDSYGATPLHLAAMR GHLEIVEVLLKYGADVNAADEEGATPLHLAAKAGHLEIVE VLLKNGADVNAQDKFGKTAFDISIDNGNEDLAEILQKLgsgsg ggsgss <u>RDHMLHEYVNAAGIT</u> sgsggsLPETGGG	24.23	3.90
DARPinK27-D30-HiBiT	MDLGKKLLEAARAGQDDEVRLMANGADVNAHDTFGFTP LHLAALYGHLEIVEVLLKNGADVNADDSYGRTPHLAAMR GHLEIVEVLLKYGADVNAADEEGRTPLHLAAKRGHLEIVEV LLKNGADVNAQDKFGKTAFDISIDNGNEDLAEILQKLgsgsgg gss <u>VSGWRLFVKKIS</u> sgsggsLPETGGG	23.95	4.02
DARPinK27n3-D30-HiBiT	MDLGKKLLEAARAGQDDEVRLMANGADVNAHDTFGFTP LHLAALYGHLEIVEVLLKNGADVNADDSYGATPLHLAAMR GHLEIVEVLLKYGADVNAADEEGATPLHLAAKAGHLEIVE VLLKNGADVNAQDKFGKTAFDISIDNGNEDLAEILQKLgsgsg ggsgss <u>VSGWRLFVKKIS</u> sgsggsLPETGGG	23.70	3.92

3G124-D30-S11	MDLGKKLLEAARAGQDDEVRLMANGADVNAADDVGVTP LHLAAQRGHLEIVEVLLKYGADVNAADLWGQTPHLAAT AGHLEIVEVLLKNGADV NARDNIGHTPLHLAAWAGHLEIV EVLLKYGADVNAQDKFGKTPFDL AIDNGNEDIAEVLQKAA ggsgggssDDDDDDDDDDDDDDDDDDDDDDDDDDDDDDssg ggsggRDHMLHEYVNAAGITsgsggsLPETGGG	24.29	3.92
gc_R7-D30-S11	MDLGKKLLEAARAGQDDEVRLMANGADVNAADDVGVTP LHLAAQRGHLEIVEVLLKYGADVNAADLWGQTPHLAAT AGHLEIVEVLLKNGADV NARDNIGHTPLHLAAWAGHLEIV EVLLKYGADVNAQDKFGKTPFDL AIDNGNEDIAEVLQKAA GGSGGGDVNAYDEVGWTPHRAAWGHLELVEKLLKNG ADVNAADIDGYTPHLAAFSGHLEIVEVLLKYGADV NADD QAGFTPLHLAAIFGHLEIVEVLLKNGADVNAQDKFGKTPFD LAIDNGNEDIAEVLQKAggsgggssDDDDDDDDDDDDDDDD DDDDDDDDDDDDDDssggsggRDHMLHEYVNAAGITsgsg gsLPETGGG	38.63	4.06
Omomyc-S11	MATEENVKRRTHNVLERQRRNELKRSFFALRDQIPELENNE KAPKVILKKATAYILSVQAETQKLISEIDLLRKQNEQLKHK LEQLRNCAggsgggssggsgggsggRDHMLHEYVNAAGITsg sggsLPETGGG	15.05	9.37
Omomyc-E30-S11	MATEENVKRRTHNVLERQRRNELKRSFFALRDQIPELENNE KAPKVILKKATAYILSVQAETQKLISEIDLLRKQNEQLKHK LEQLRNCAggsgggssEEEEEEEEEEEEEEEEEEEEEEEEEEEE EEEssgggsggRDHMLHEYVNAAGITsgsggsLPETGGG	18.81	4.46
aGFpnb-S11	MAGsgsgsggMDQVQLVESGGALVQPGGSLRLSCAASGFPV NRYSMRWYRQAPGREREWVAGMSSAGDRSSYEDSVRGRF TISRDDARNTVYLQMNSLRPEDTAVYYCNVNVGFYWGQ GTQVTVssggsgggssggsgggsggRDHMLHEYVNAAGITsgsg gsLPETGGG	18.03	5.64
aGFpnb-D25-S11	MAGsgsgsggMDQVQLVESGGALVQPGGSLRLSCAASGFPV NRYSMRWYRQAPGREREWVAGMSSAGDRSSYEDSVRGRF TISRDDARNTVYLQMNSLRPEDTAVYYCNVNVGFYWGQ GTQVTVssggsgggssDDDDDDDDDDDDDDDDDDDDDDDDDD ssggsggRDHMLHEYVNAAGITsgsggsLPETGGG	20.79	3.91
aTaqAffibody-S11	MVDNKFNKELGWATWEIFNLPNLNGVQVKAFIDSLRDDPS QSANLLAEAKKLNDQAQPKggsgggssggsgggsggRDHML HEYVNAAGITsgsggsLPETGGG	10.79	5.16
aTaqAffibody-D30-S11	MVDNKFNKELGWATWEIFNLPNLNGVQVKAFIDSLRDDPS QSANLLAEAKKLNDQAQPKggsgggssDDDDDDDDDDDDDD DDDDDDDDDDDDDDssggsggRDHMLHEYVNAAGI TsgsggsLPETGGG	14.13	3.62

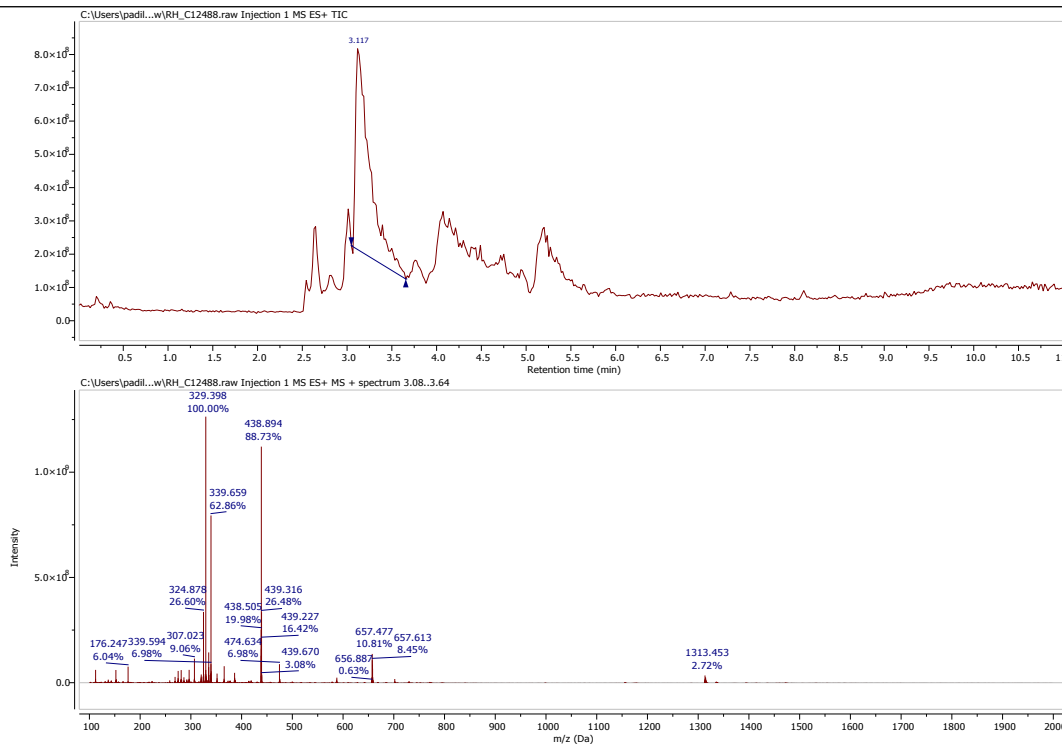
Table S2. Structure diagrams and characterization of ionizable lipids used in this work.

Lipid Identifier	Structure and Spectra	Comments
C12-200	 <p style="text-align: center;">C12-200</p>	
C12-113	 <p style="text-align: center;">C12-113</p>	
C12-1	 <p style="text-align: center;">C12-1</p>	

C12-2

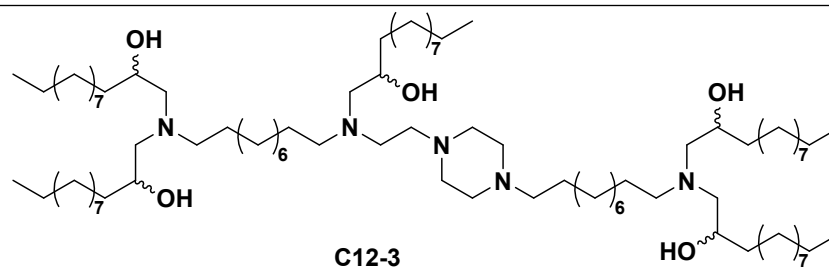


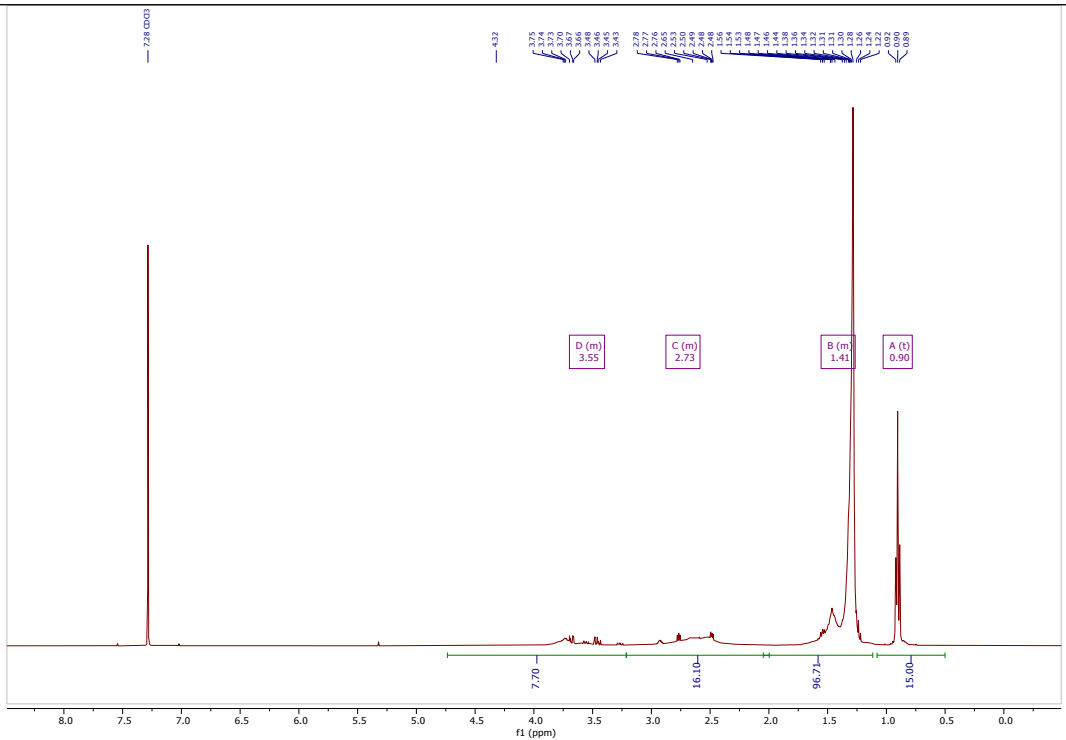
¹H NMR
(400
MHz,
CDCl₃) δ
4.51 –
3.14 (m,
23H), 3.04
– 1.95 (m,
7H), 1.89
– 1.06 (m,
202H),
0.88 (t, *J*
= 6.7 Hz,
15H).



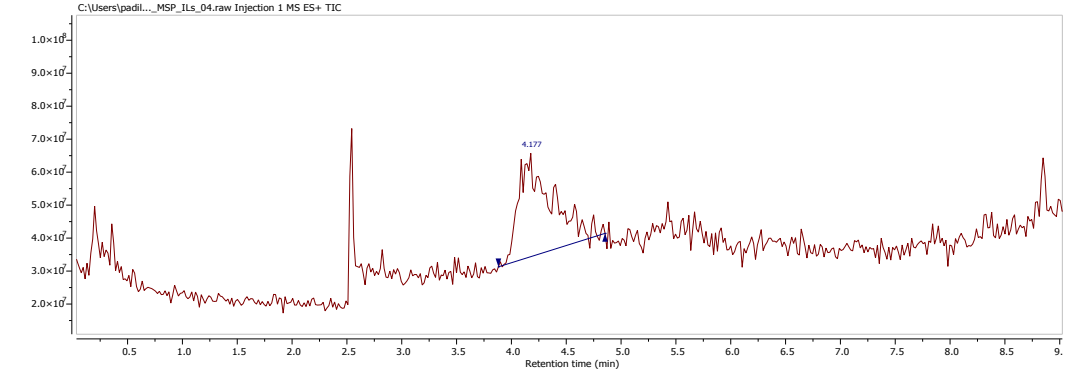
MS (ESI):
calculated
1313.16;
found
1313.45.

C12-3

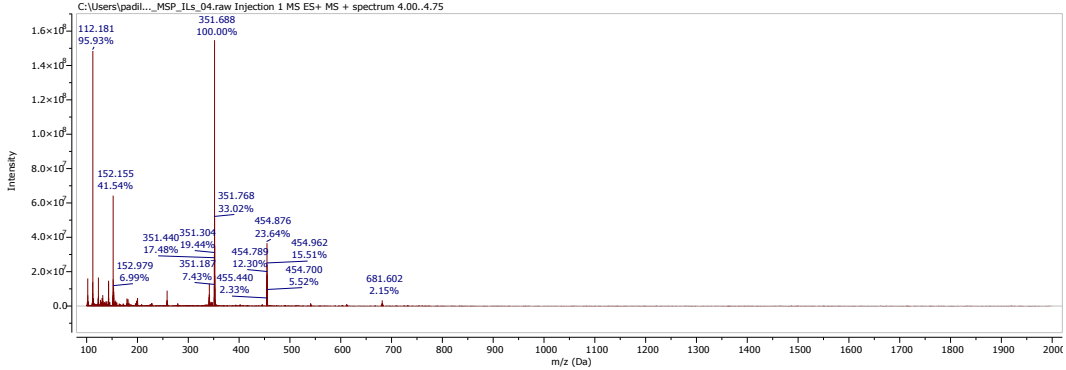




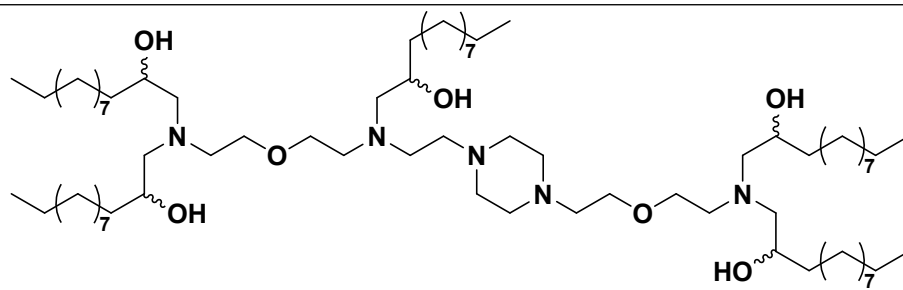
¹H NMR (400 MHz, CDCl₃) δ 4.65 – 3.10 (m, 8), 3.10 – 2.17 (m, 16H), 1.92 – 1.11 (m, 97H), 0.90 (t, *J* = 6.7 Hz, 15H).



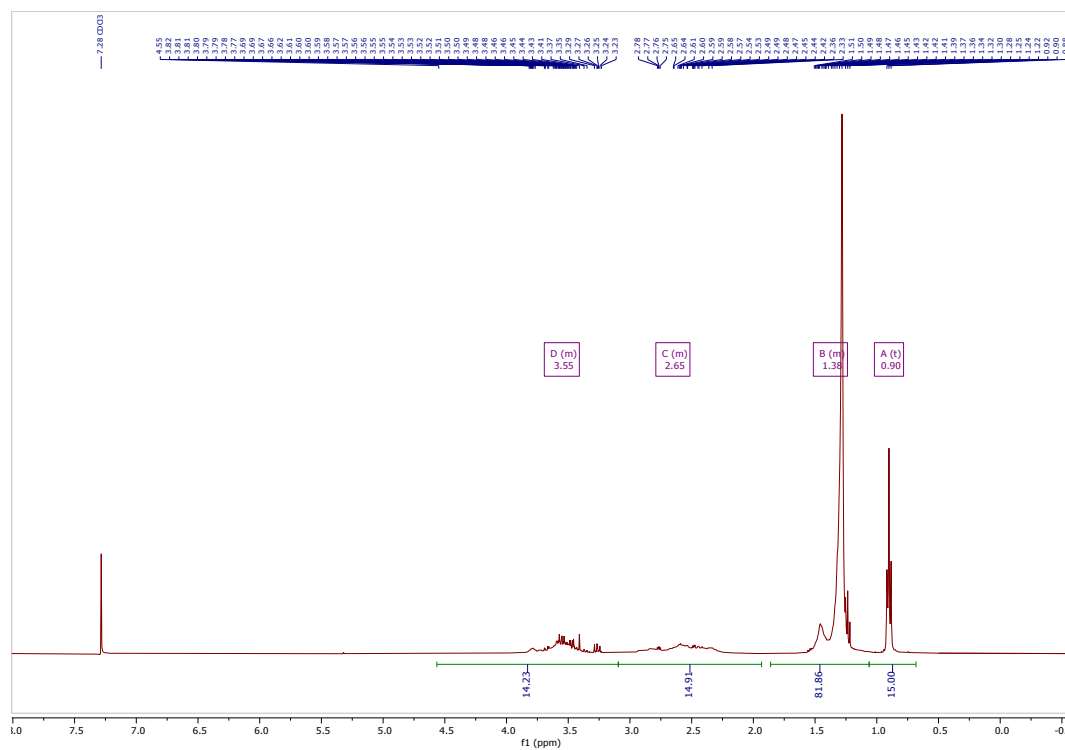
MS (ESI): calculated 1361.38; found 681.6 (m/2).



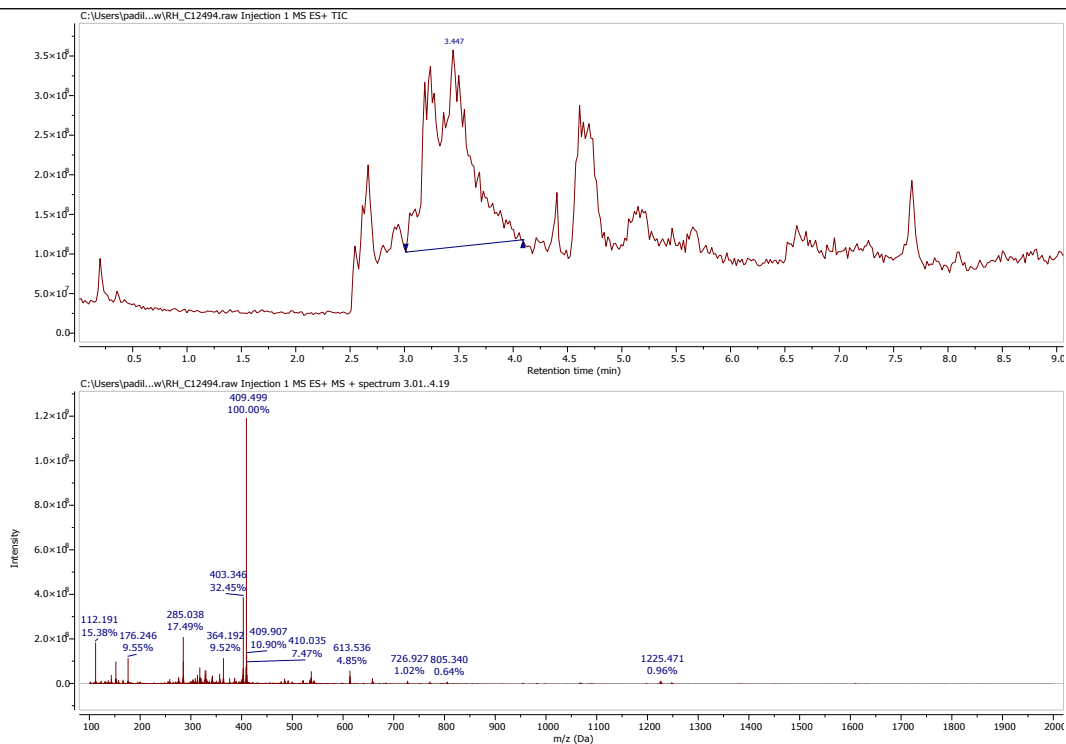
C12-4



C12-4

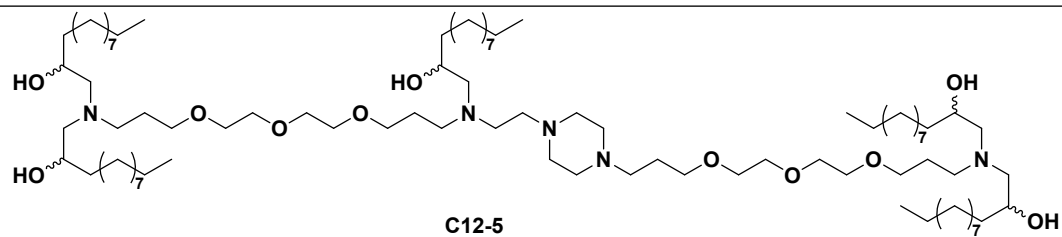


¹H NMR
(400
MHz,
CDCl₃) δ
4.68 –
3.11 (m,
14H), 3.12
– 1.98 (m,
15H), 1.83
– 1.06 (m,
82H), 0.90
(t, *J* = 6.7
Hz, 15H).

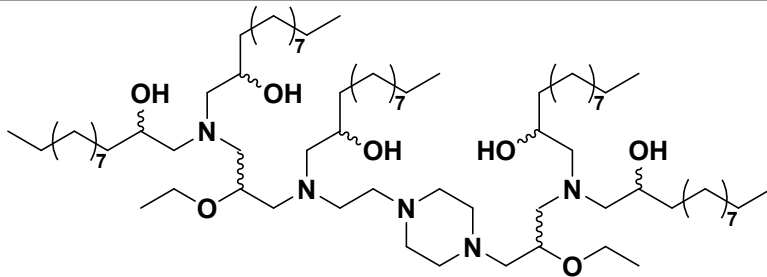


MS (ESI):
 calculated
 1225.05;
 found
 1225.47.

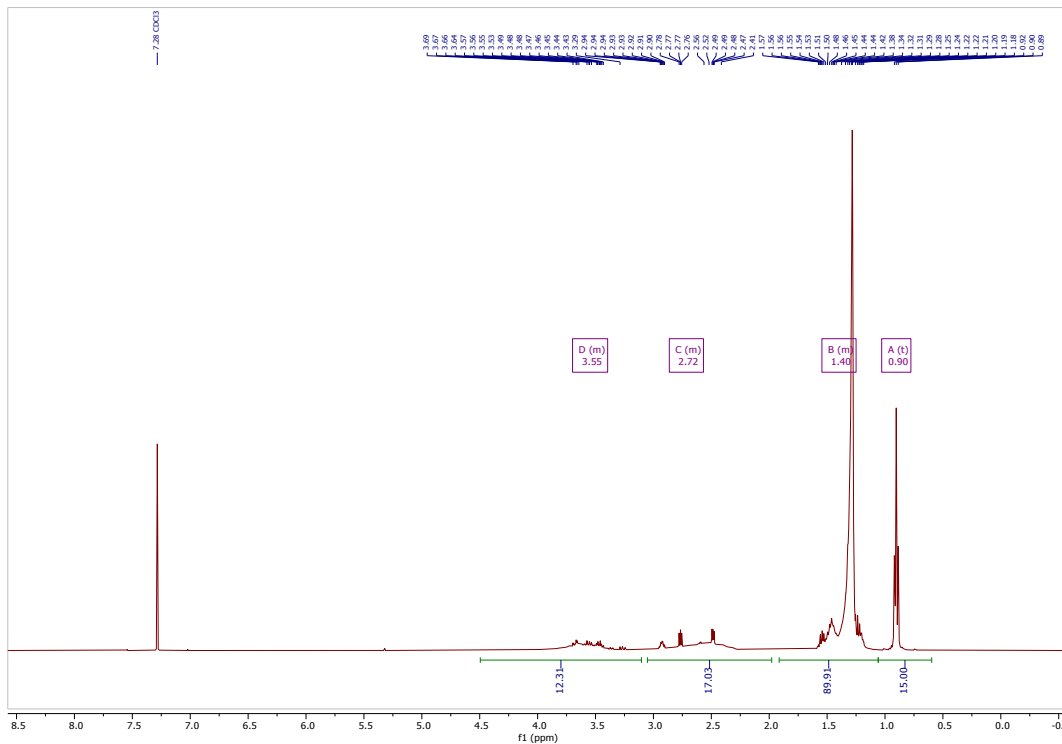
C12-5



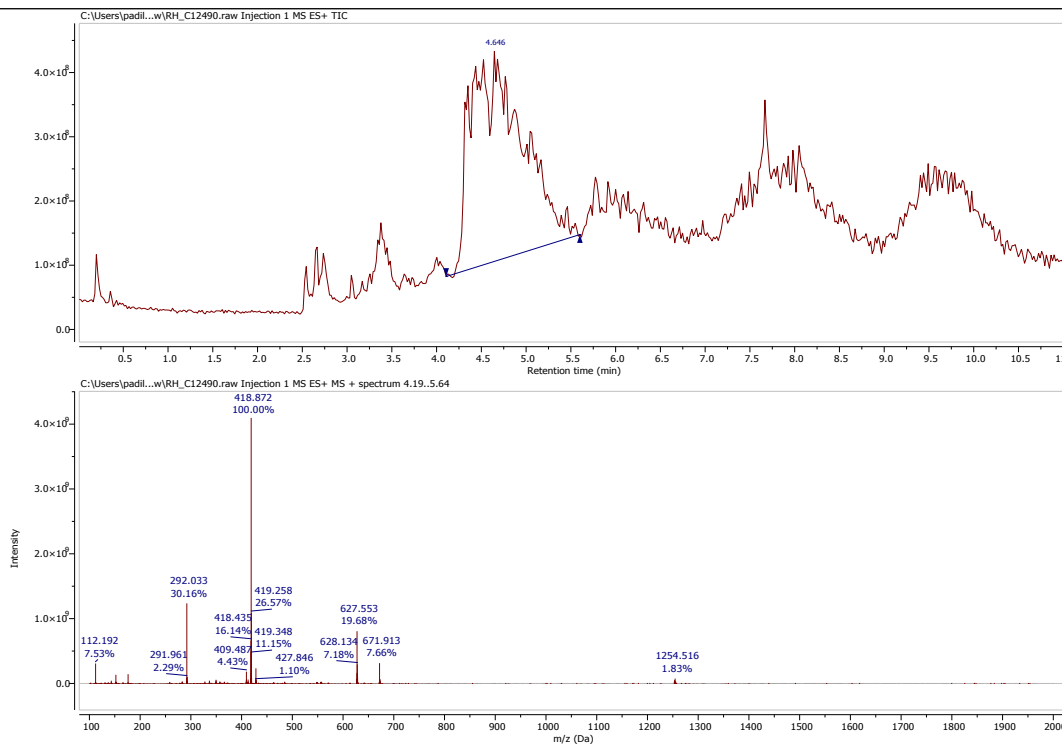
C12-6



C12-6

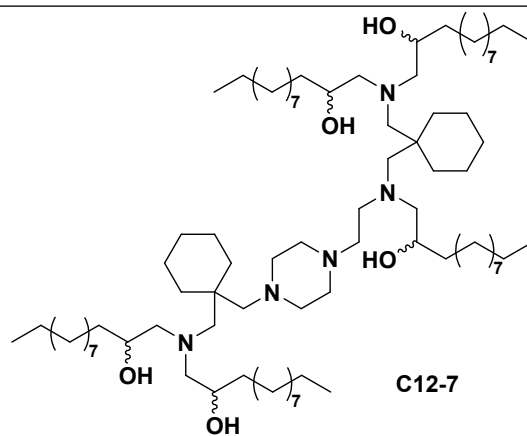


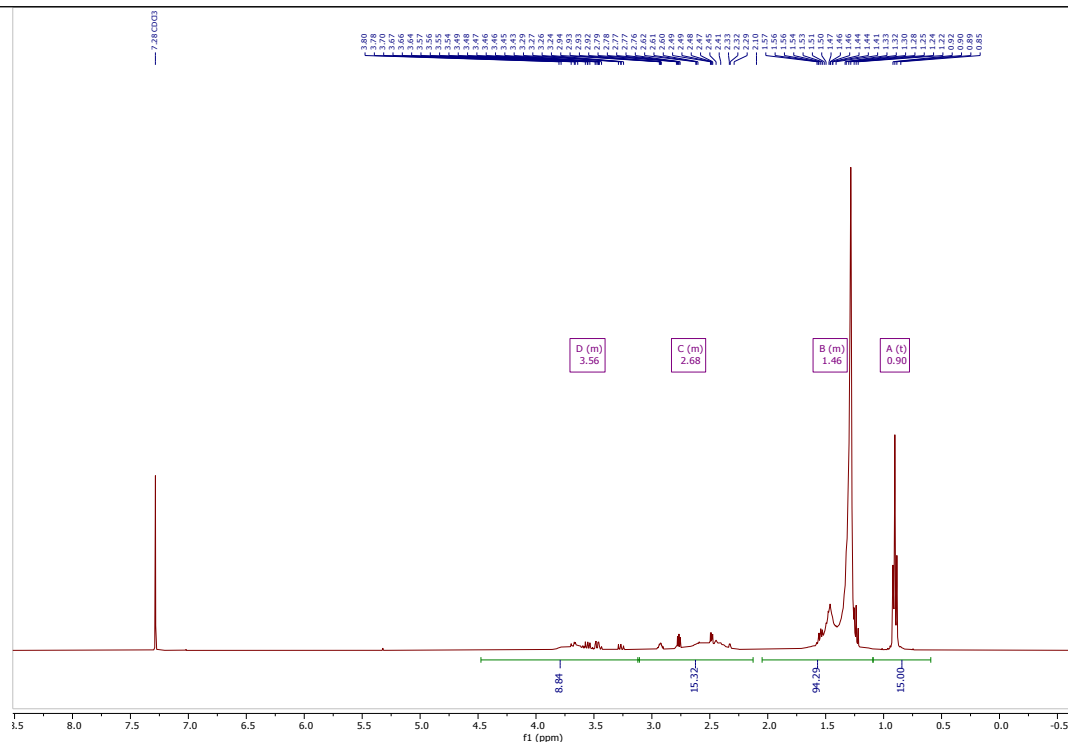
¹H NMR
(400
MHz,
CDCl₃) δ
4.85 –
3.11 (m,
12H), 3.16
– 1.97 (m,
17H), 1.97
– 1.03 (m,
90H), 0.90
(t, *J* = 6.7
Hz, 15H).



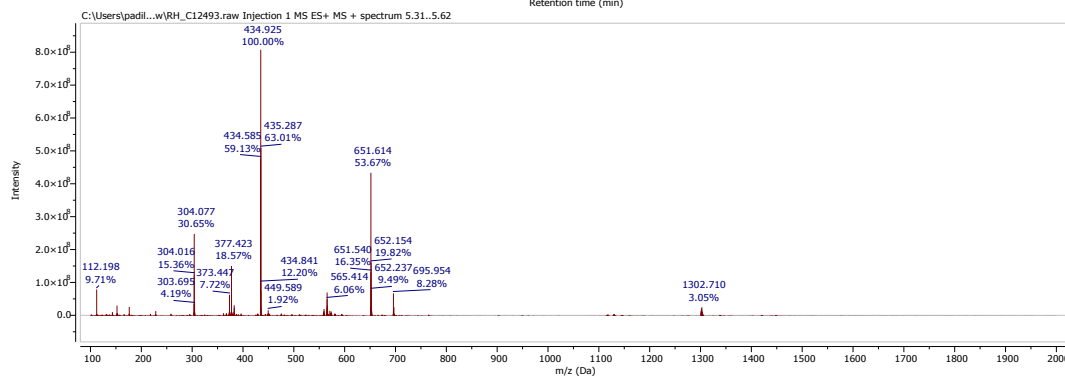
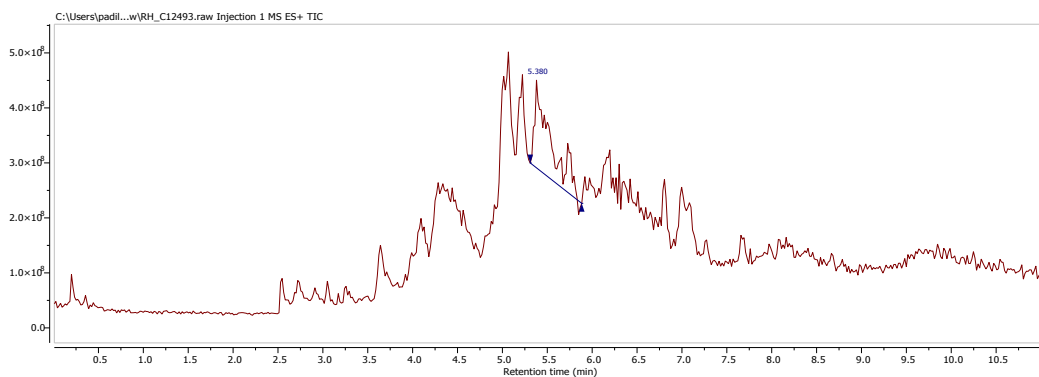
MS (ESI):
 calculated
 1253.11;
 found
 1254.52.

C12-7



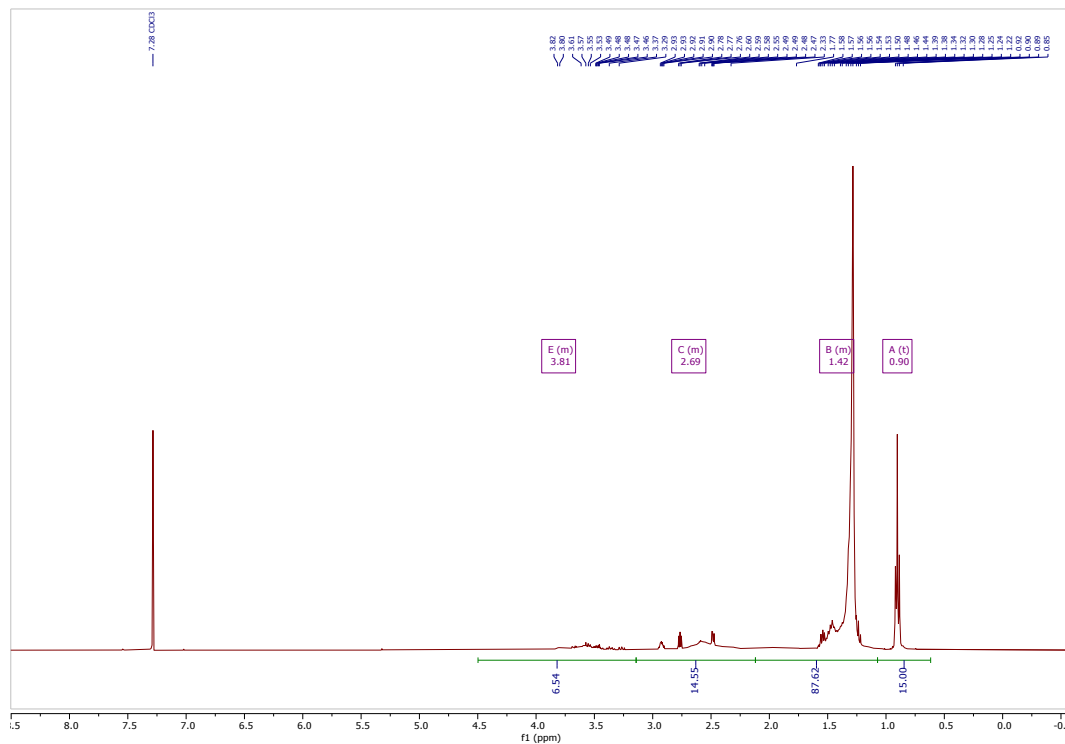
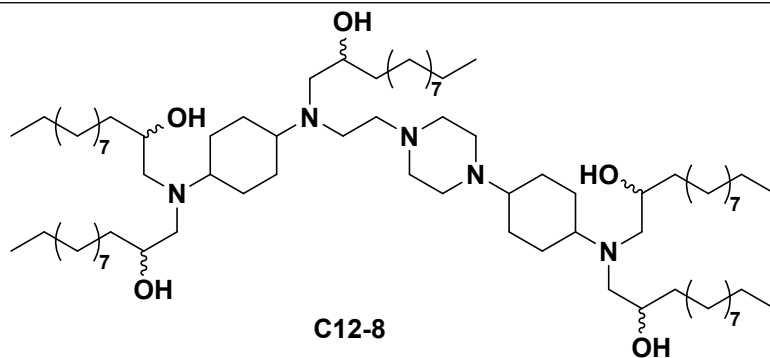


¹H NMR
(400 MHz, CDCl₃) δ
4.56 – 3.10 (m, 9H), 3.10 – 2.06 (m, 15H), 2.04 – 1.07 (m, 94H), 0.90 (t, *J* = 6.7 Hz, 15H).

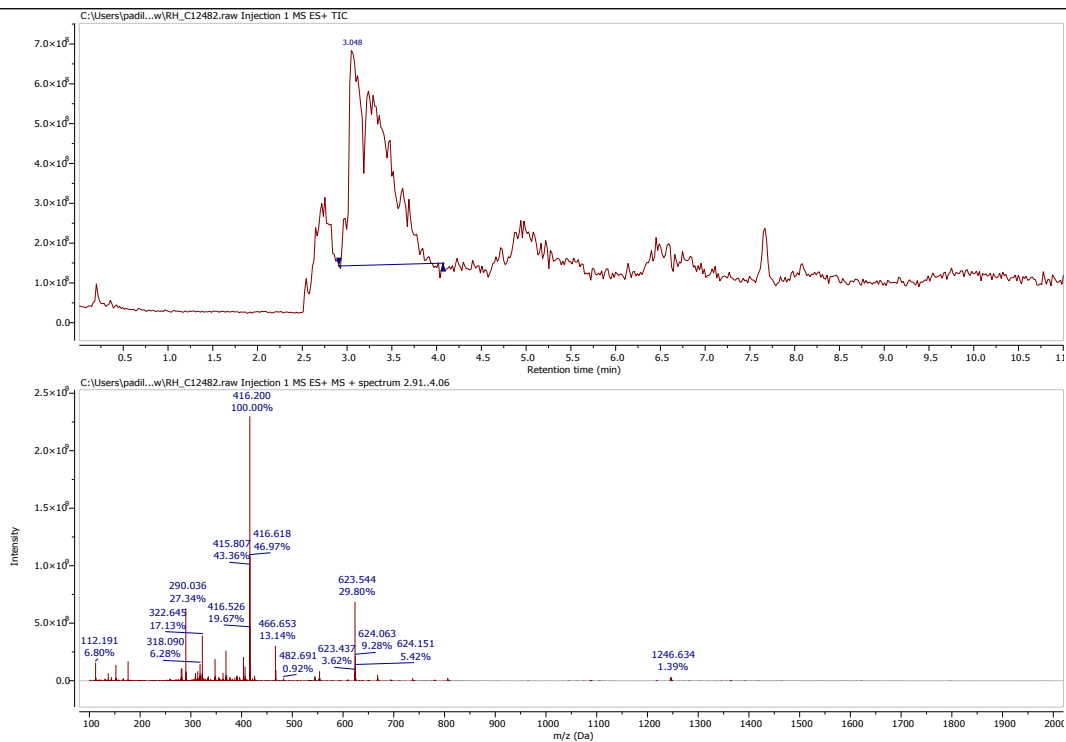


MS (ESI):
calculated
1301.24;
found
1302.71.

C12-8

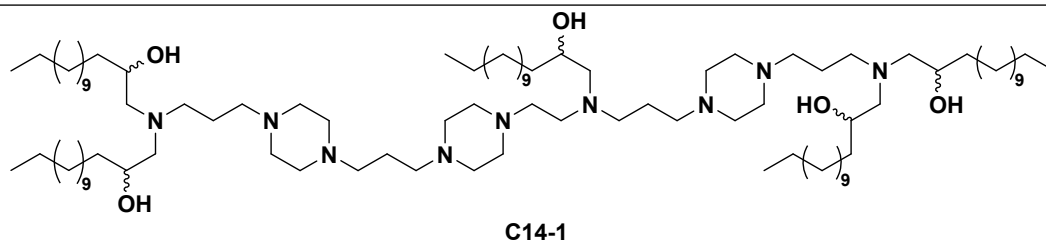


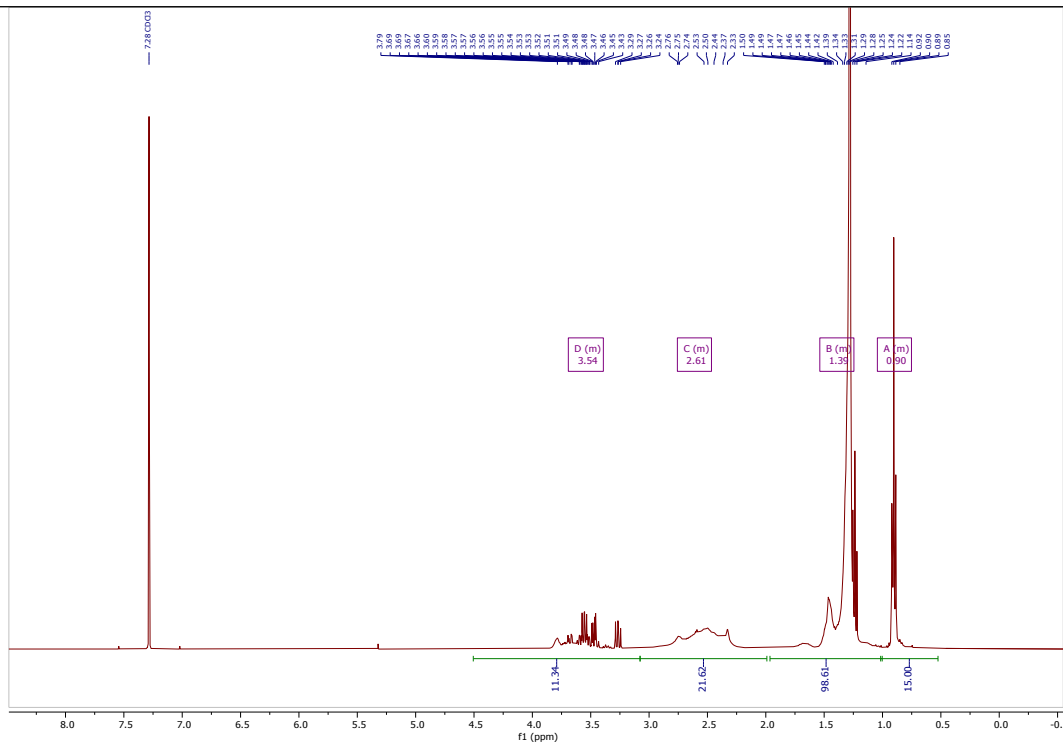
¹H NMR
(400
MHz,
CDCl₃) δ
4.28 –
3.23 (m,
6H), 3.14
– 2.12 (m,
15H), 2.12
– 1.05 (m,
88H), 0.90
(t, *J* = 6.7
Hz, 15H).



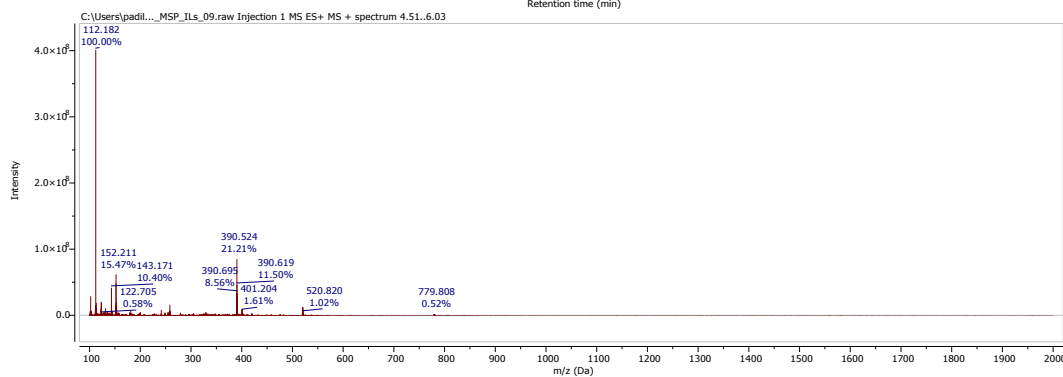
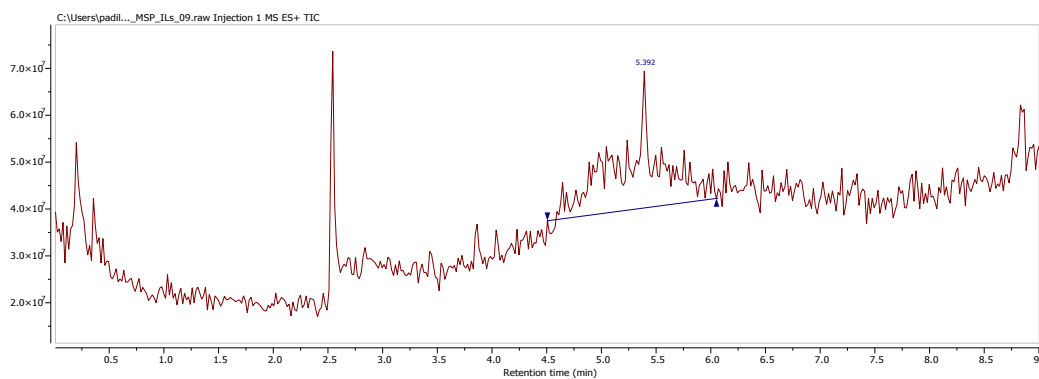
MS (ESI):
 calculated
 1244.90;
 found
 1246.63.

C14-1



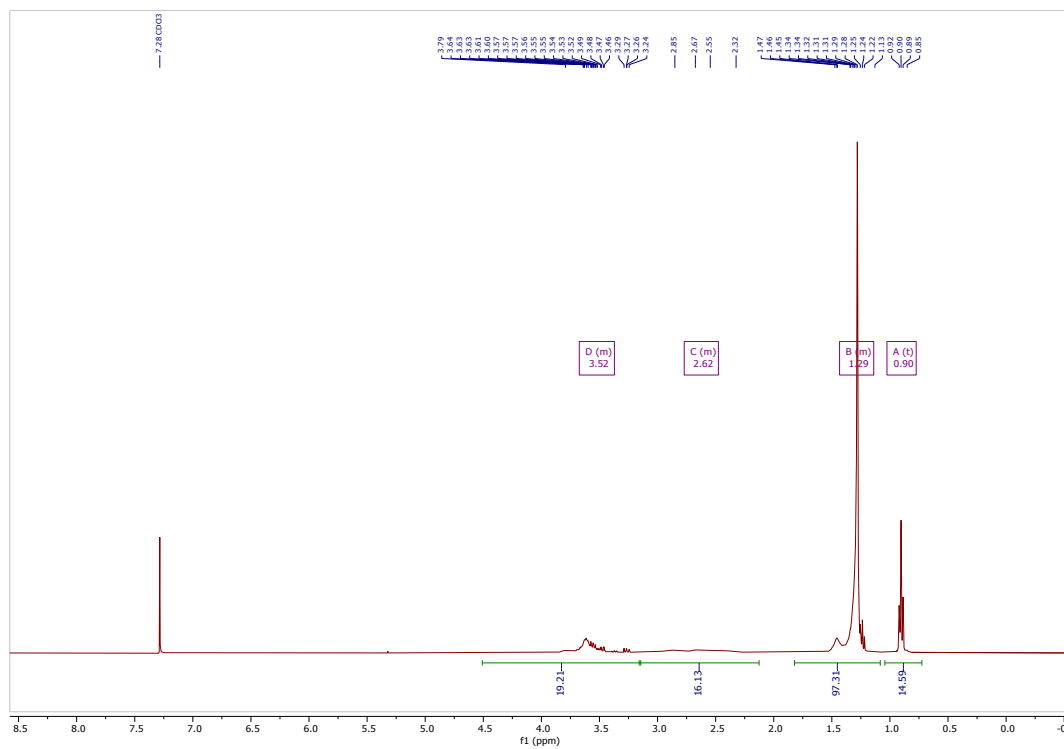
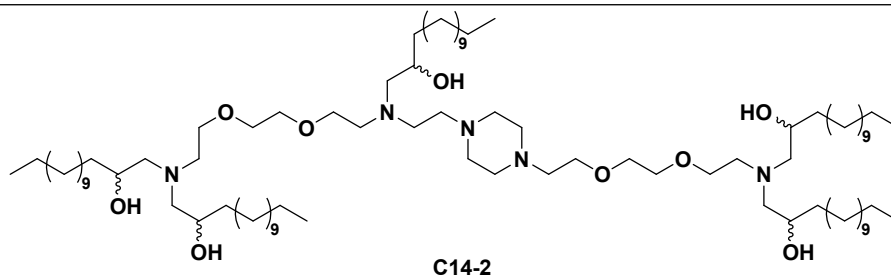


¹H NMR
(400
MHz,
CDCl₃) δ
4.50 –
3.07 (m,
11H), 3.04
– 2.01 (m,
22H), 1.94
– 0.99 (m,
99H), 0.96
– 0.85 (m,
15H).

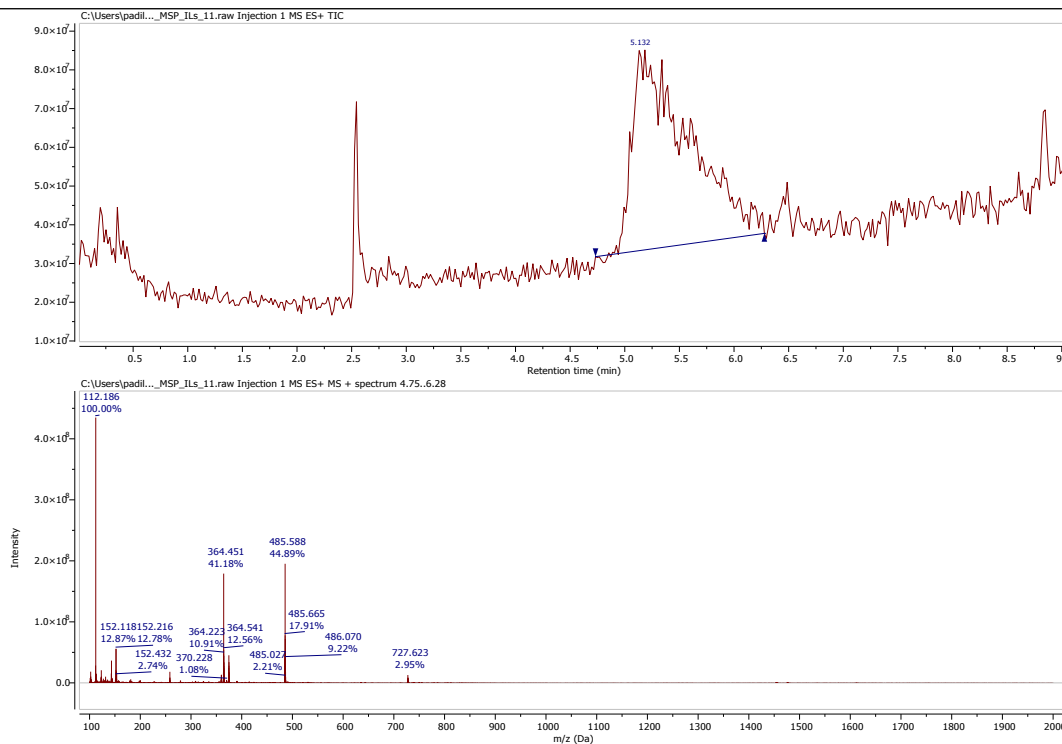


MS (ESI):
calculated
1557.66;
found
779.81
(m/2).

C14-2

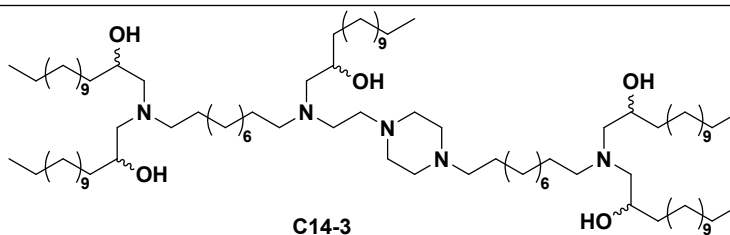


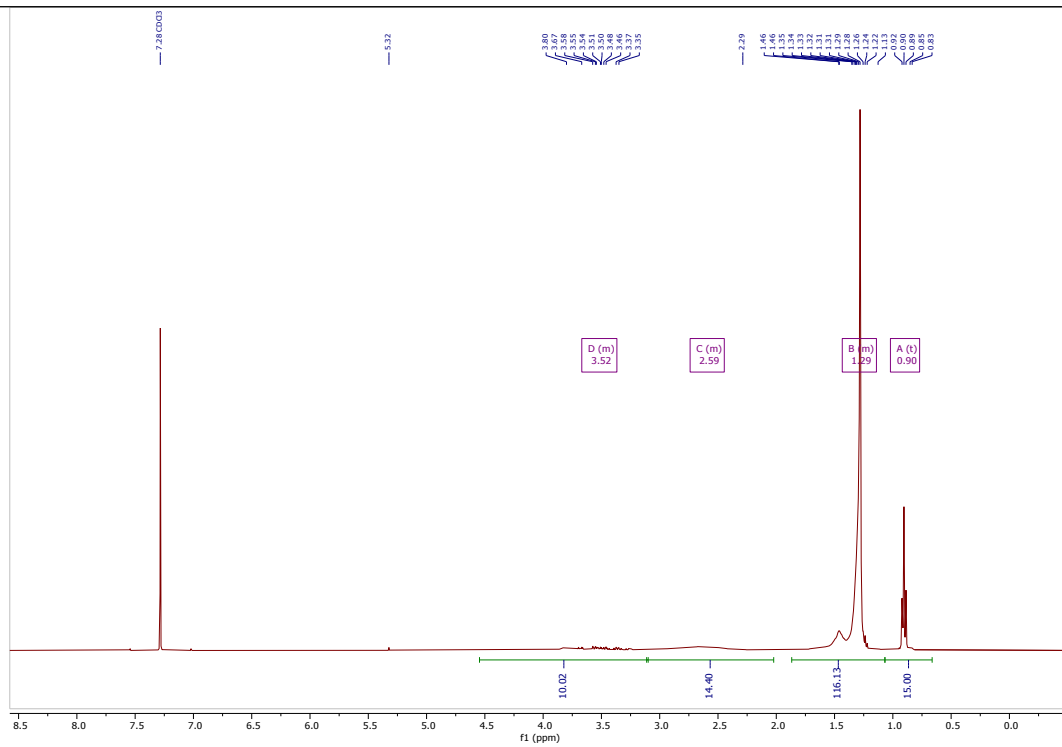
¹H NMR
(400
MHz,
CDCl₃) δ
4.50 –
3.09 (m,
19H), 3.11
– 1.96 (m,
16H), 1.84
– 1.08 (m,
97H), 0.90
(t, 15H).



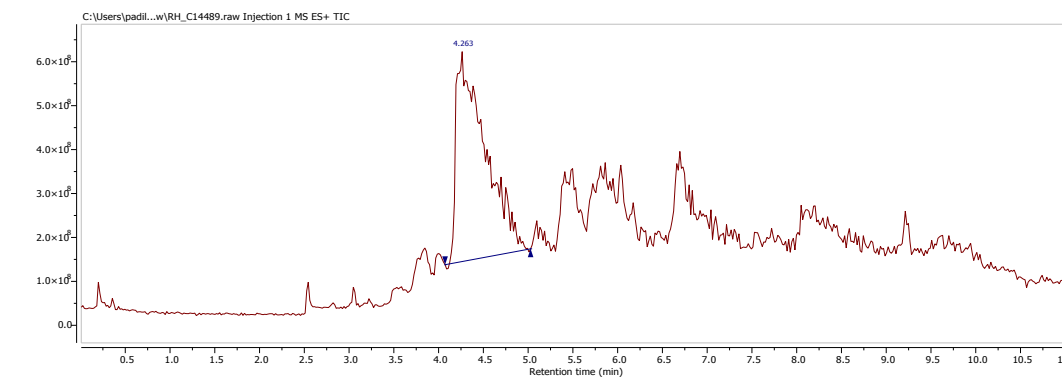
MS (ESI):
 calculated
 1453.41;
 found
 727.62
 (m/2).

C14-3

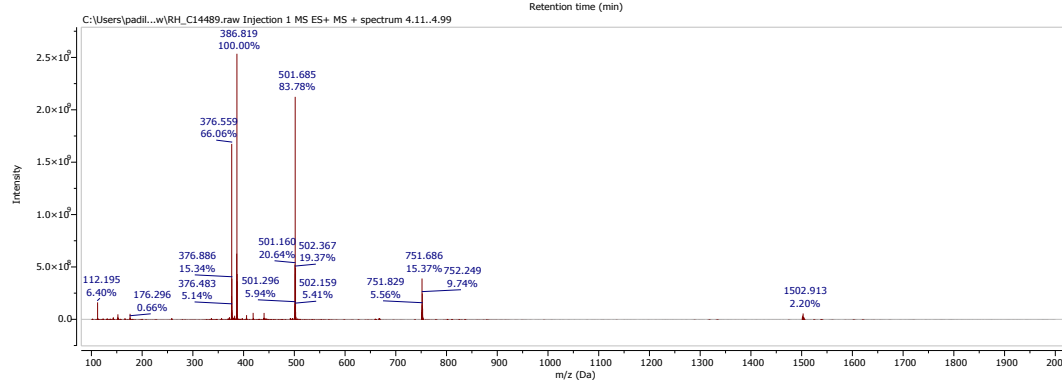




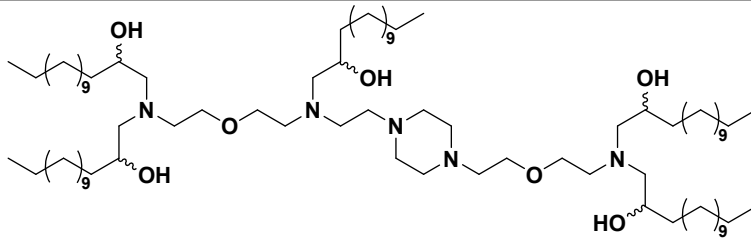
¹H NMR (400 MHz, CDCl₃) δ 4.51 – 3.20 (m, 10H), 3.18 – 1.98 (m, 14H), 1.84 – 1.11 (m, 116H), 0.90 (t, 15H).



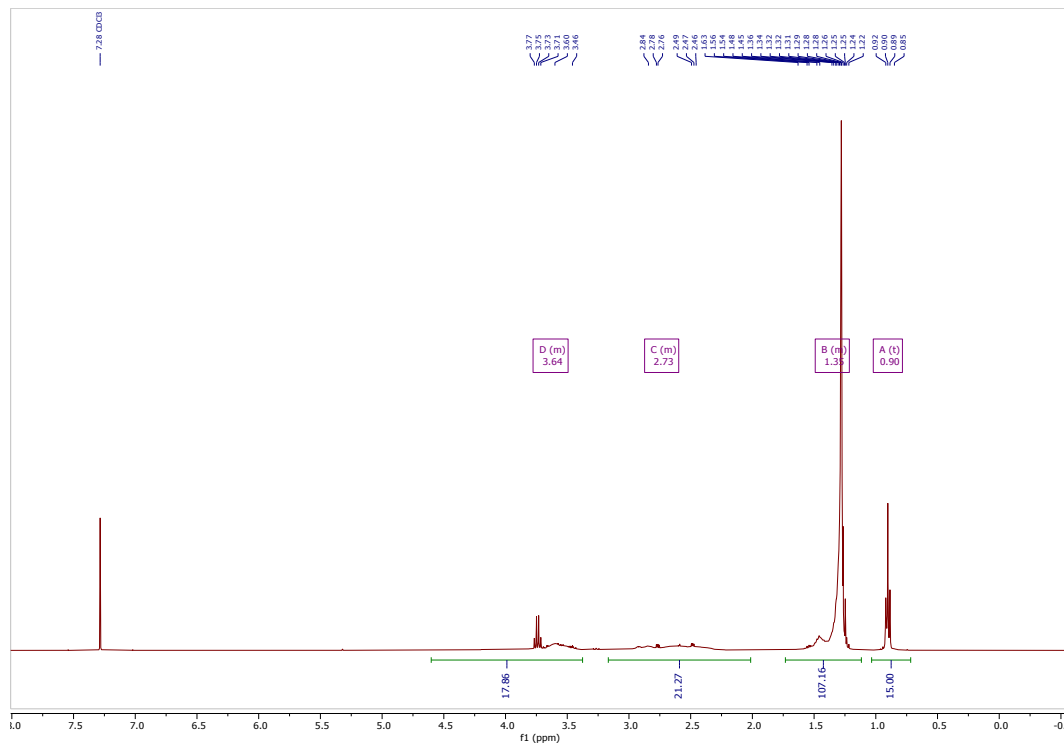
MS (ESI):
calculated 1501.63;
found 1502.91.



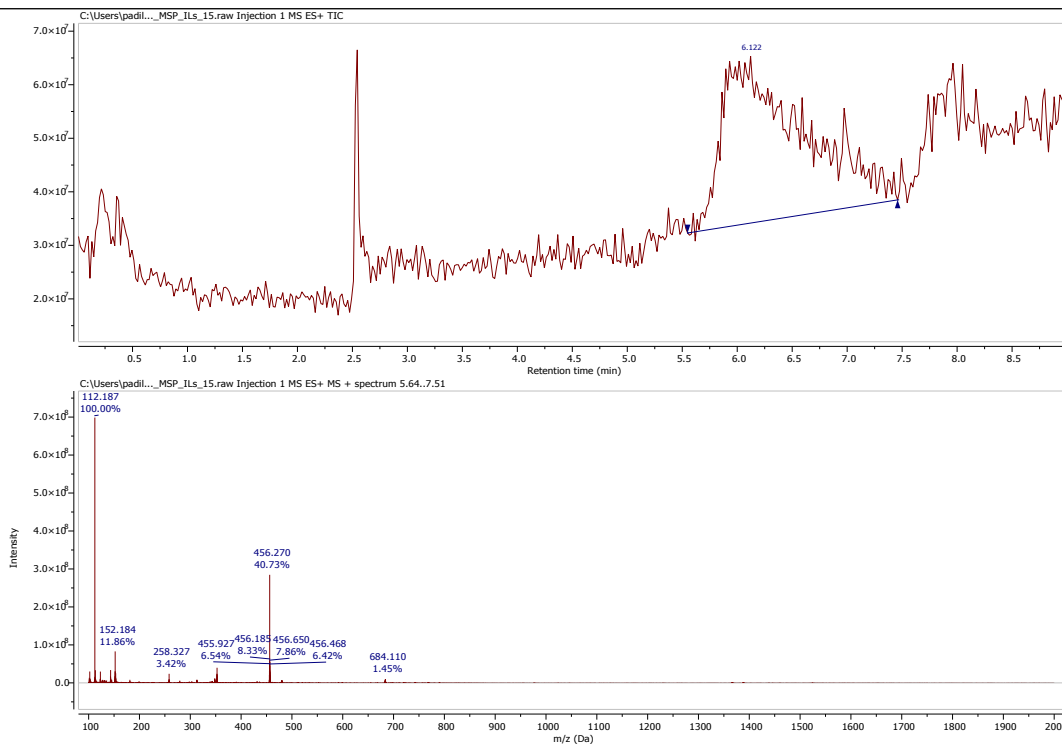
C14-4



C14-4

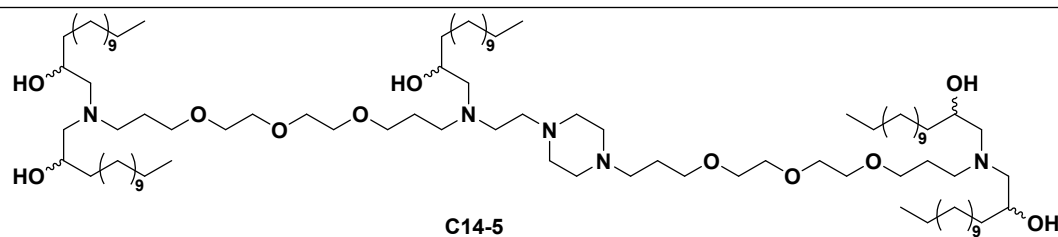


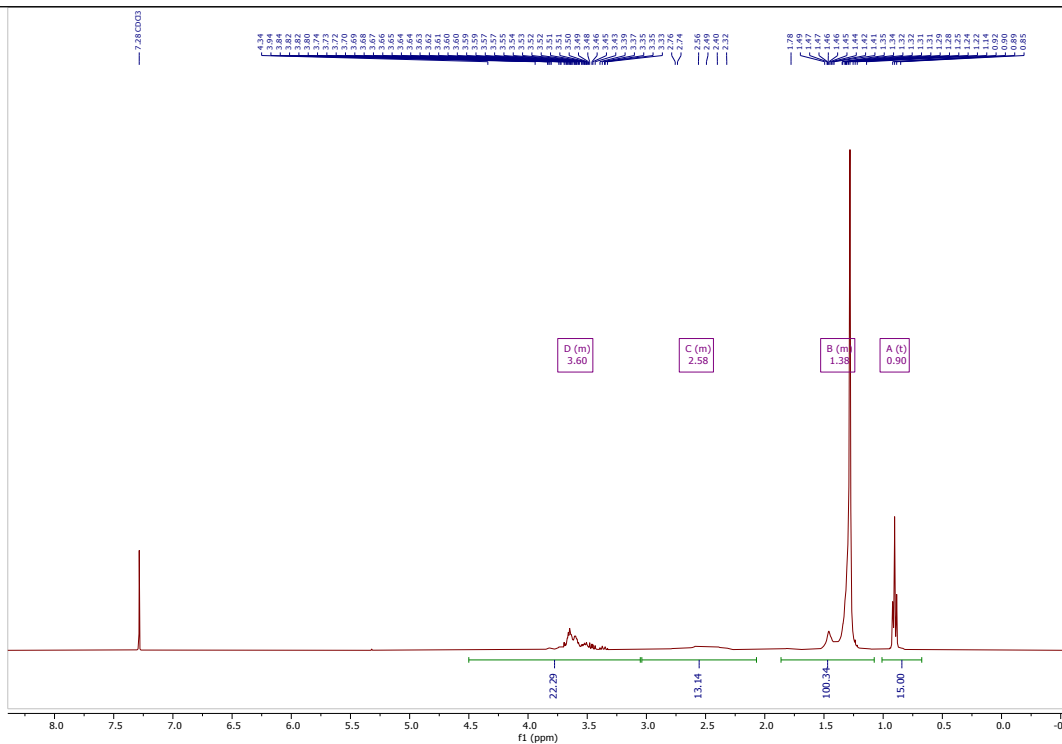
¹H NMR
(400
MHz,
CDCl₃) δ
4.65 –
3.35 (m,
18H), 3.13
– 2.05 (m,
21H), 1.80
– 1.09 (m,
107H),
0.90 (t, *J*
= 6.8 Hz,
15H).



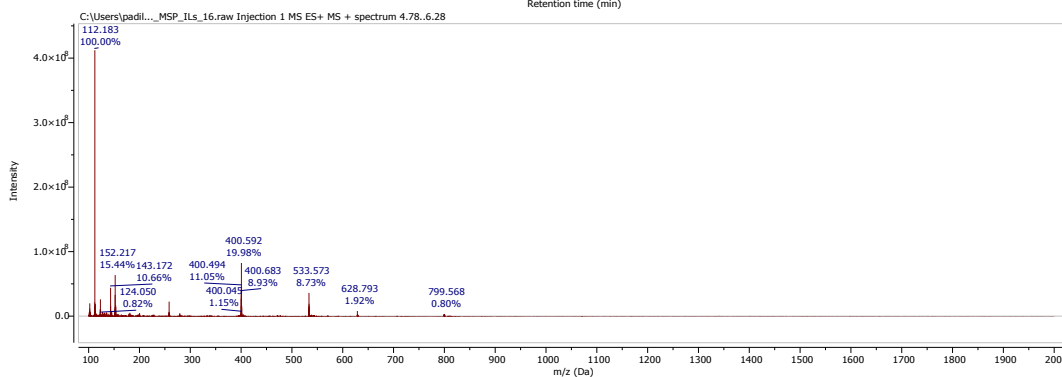
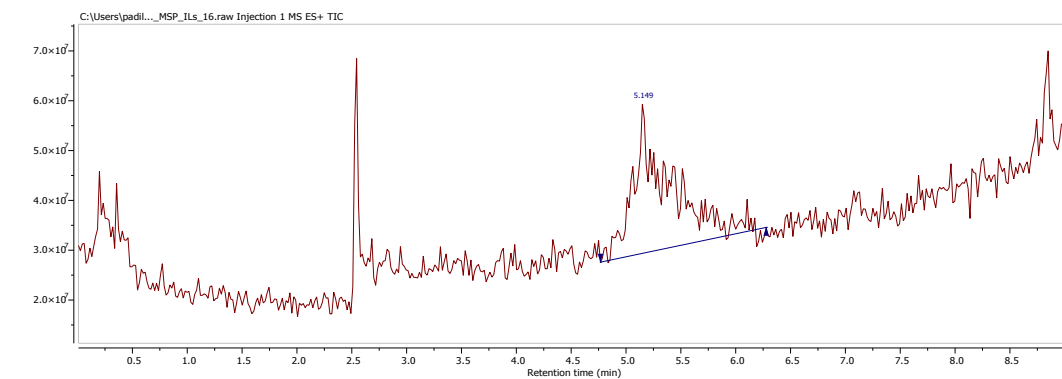
MS (ESI):
calculated
1365.30;
found
684.11
(m/2).

C14-5



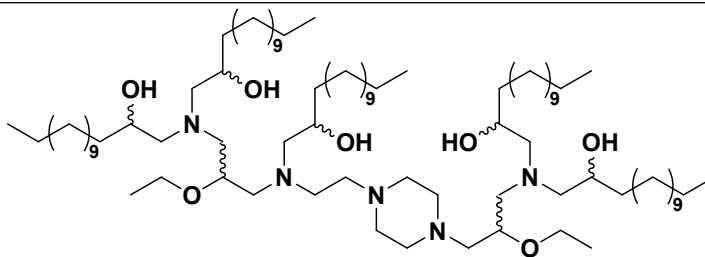


^1H NMR
(400 MHz, CDCl_3) δ
4.63 –
3.10 (m, 22H), 3.05 – 2.04 (m, 13H), 2.04 – 0.98 (m, 100H), 0.90 (t, $J = 6.8$ Hz, 15H).

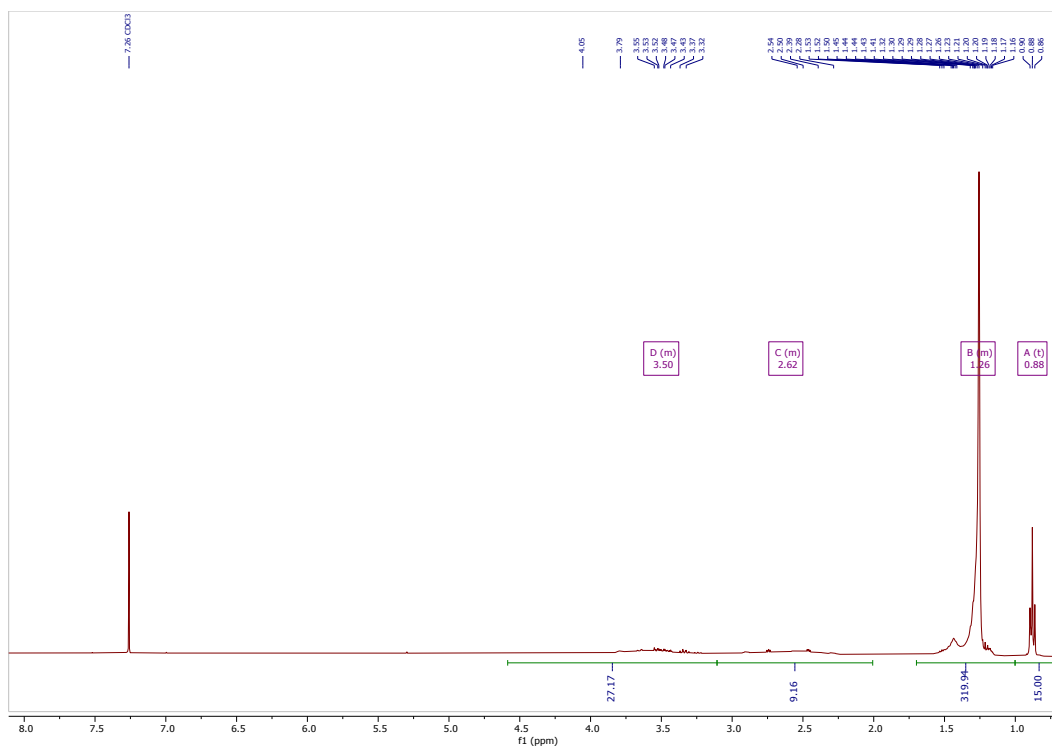


MS (ESI):
calculated
1597.62;
found
799.57
(m/2).

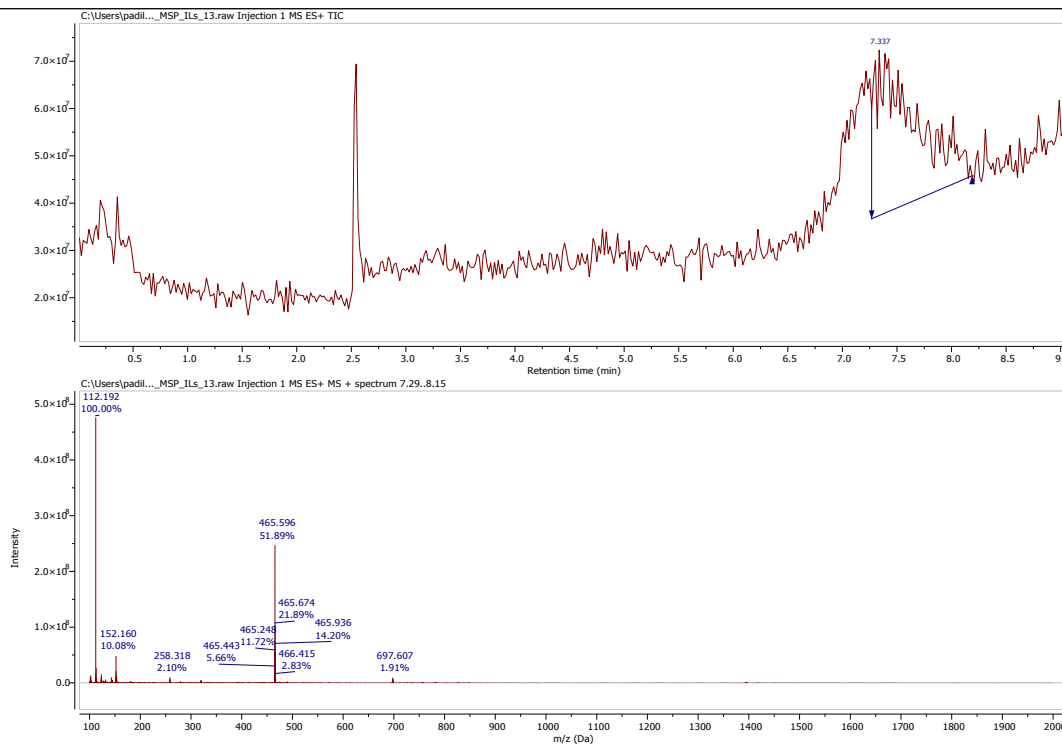
C14-6



C14-6

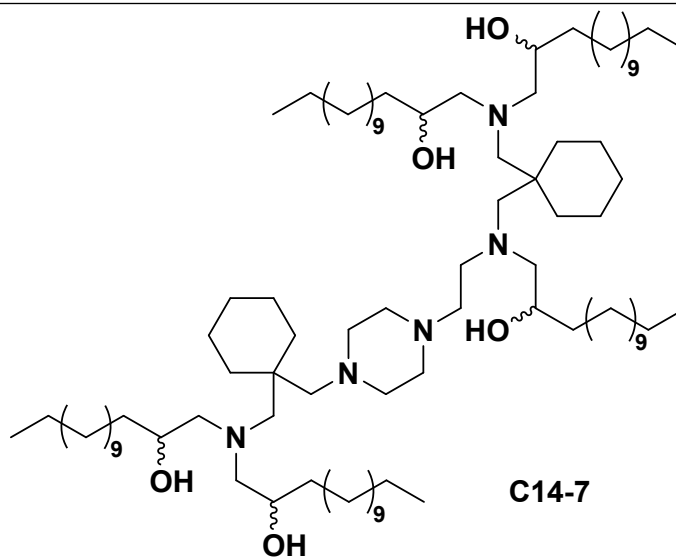


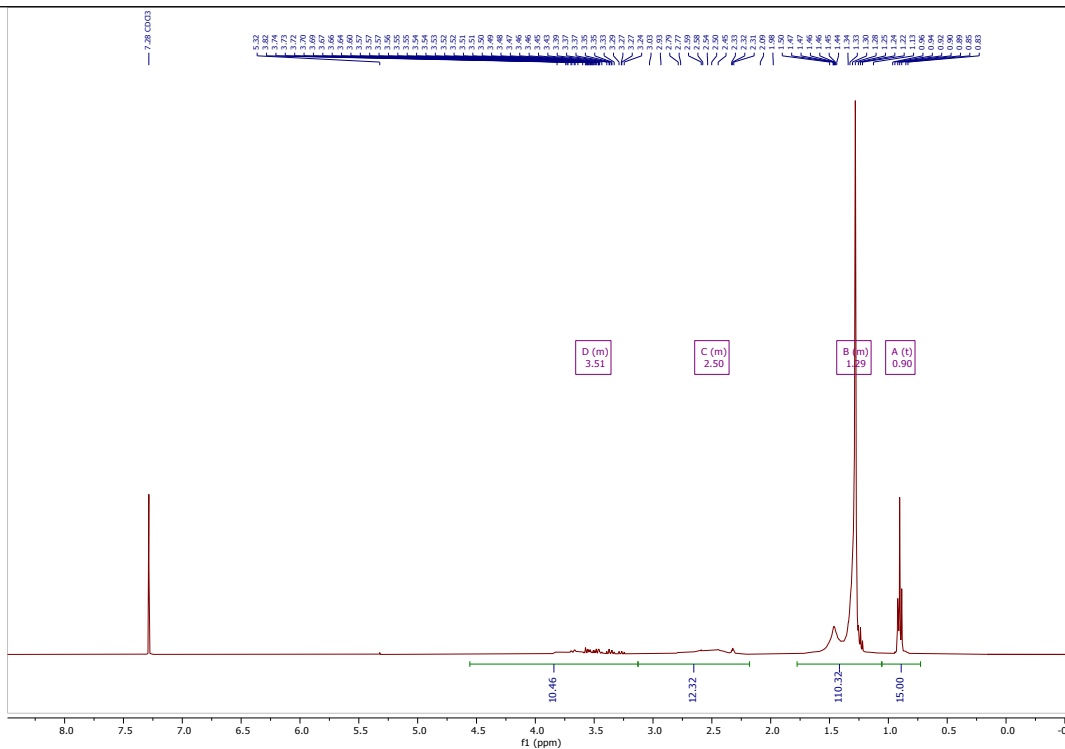
¹H NMR
(400
MHz,
CDCl₃) δ
4.34 –
3.14 (m,
27H), 3.14
– 2.03 (m,
9H), 1.70
– 1.03 (m,
320H),
0.88 (t, *J*
= 6.7 Hz,
15H).



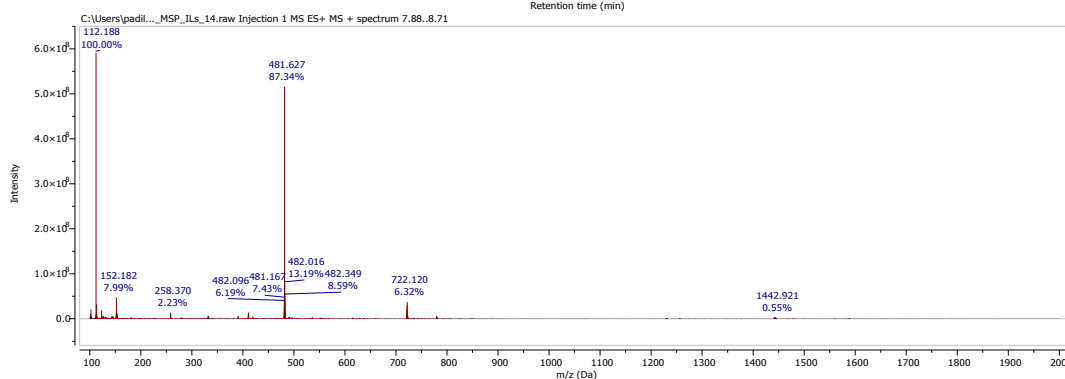
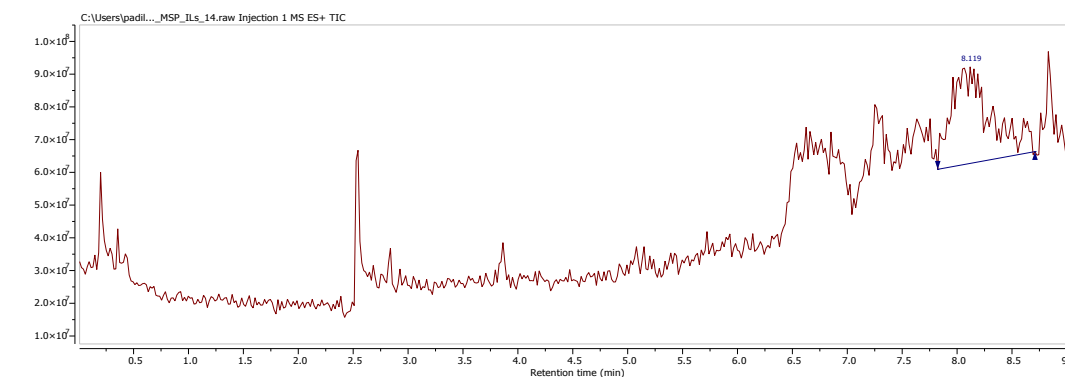
MS (ESI):
 calculated
 1393.36;
 found
 697.61
 (m/2).

C14-7



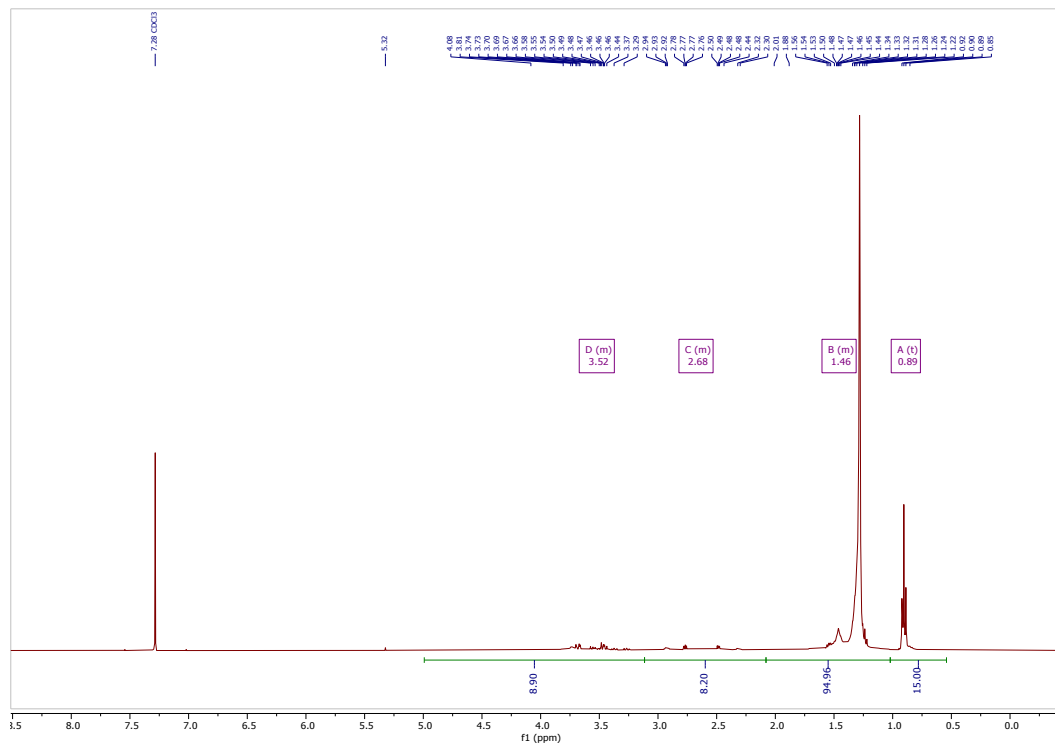
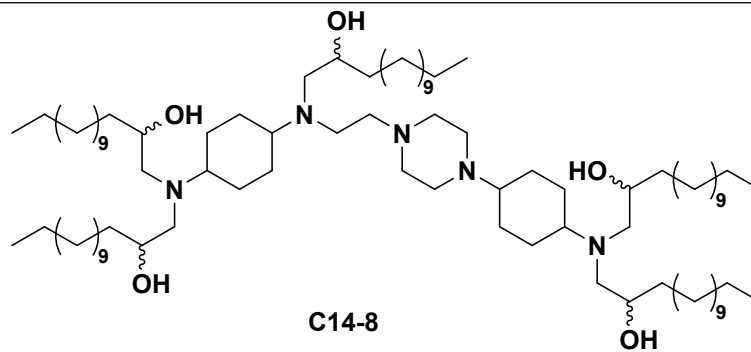


^1H NMR
 (400
 MHz,
 CDCl_3) δ
 3.98 –
 3.05 (m,
 10H), 3.12
 – 2.14 (m,
 12H), 1.73
 – 1.02 (m,
 110H),
 0.90 (t,
 15H).

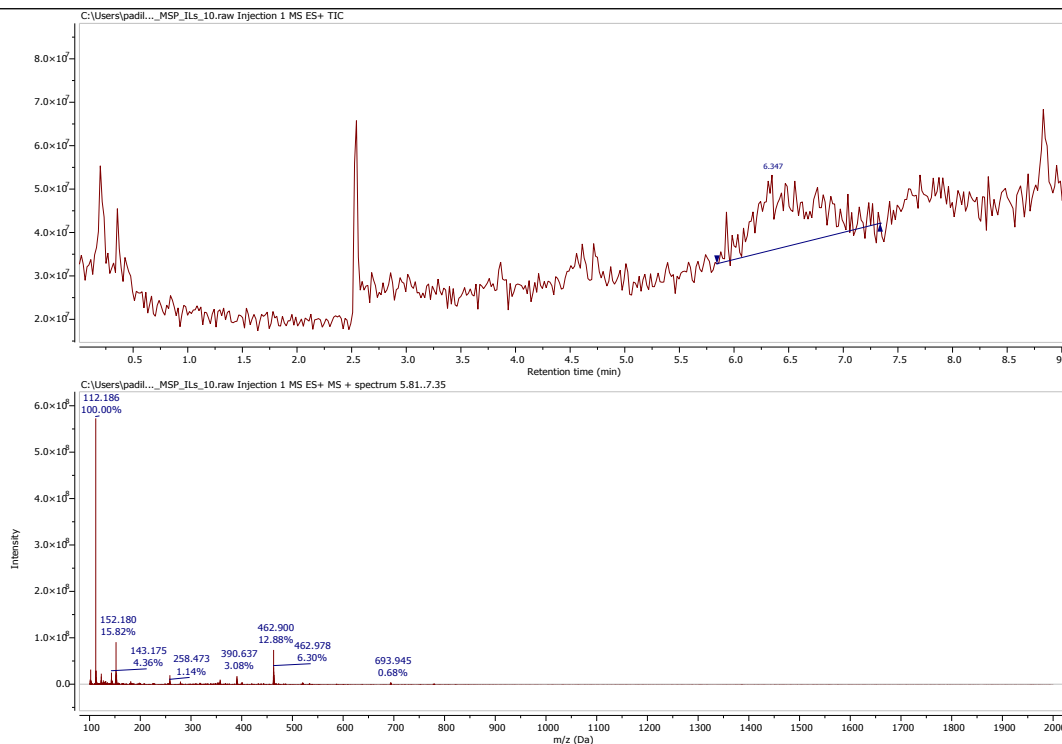


MS (ESI):
 calculated
 1441.49;
 found
 1442.91.

C14-8

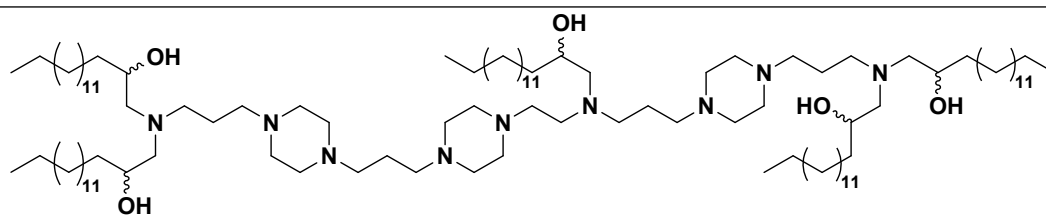


¹H NMR
(400
MHz,
CDCl₃) δ
5.02 –
3.13 (m,
9H), 3.14
– 2.12 (m,
8H), 2.08
– 1.03 (m,
95H), 0.89
(t, 15H).

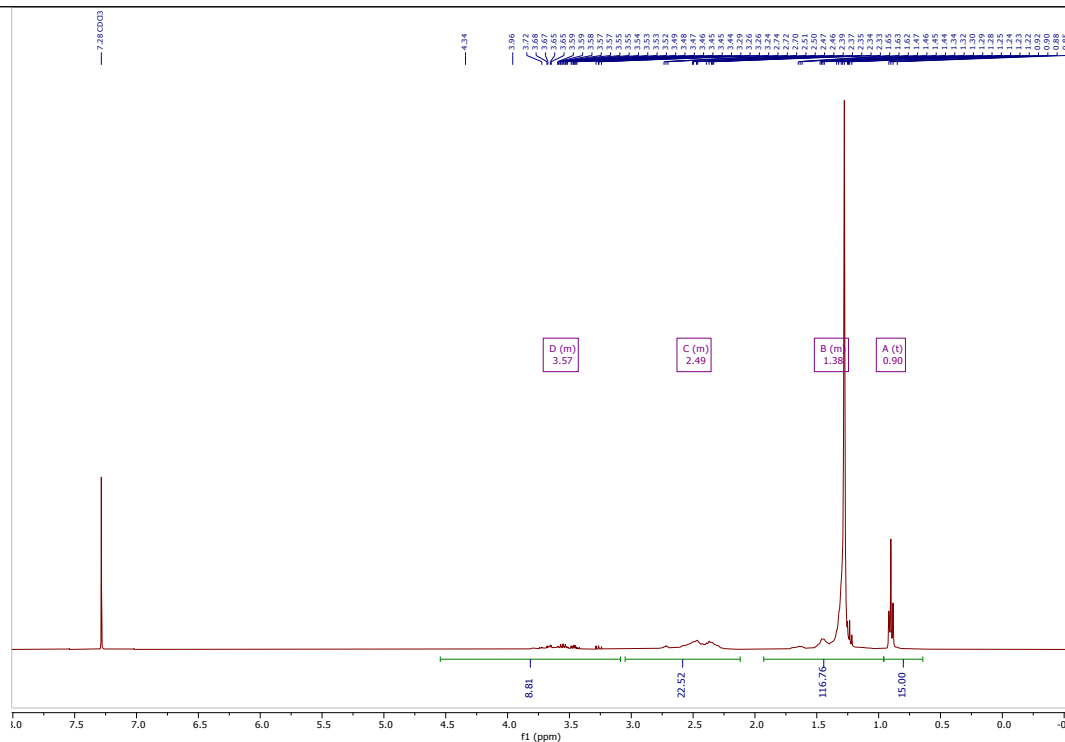


MS (ESI):
calculated
1385.15;
found
693.95
(m/2).

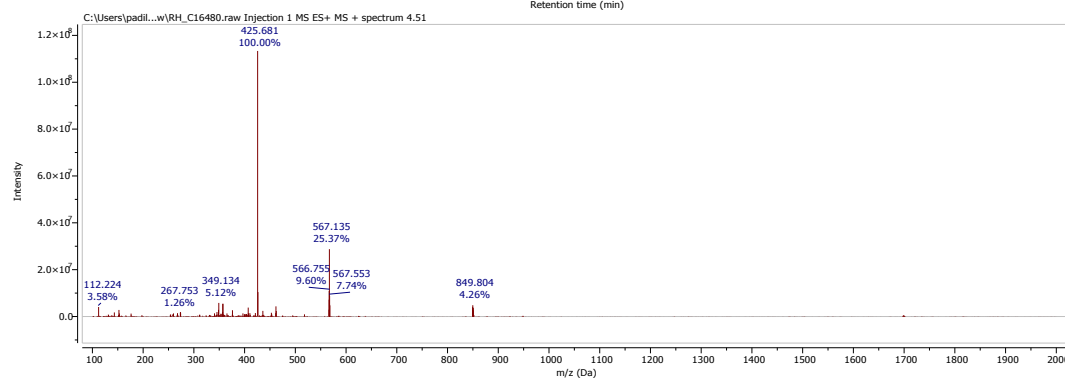
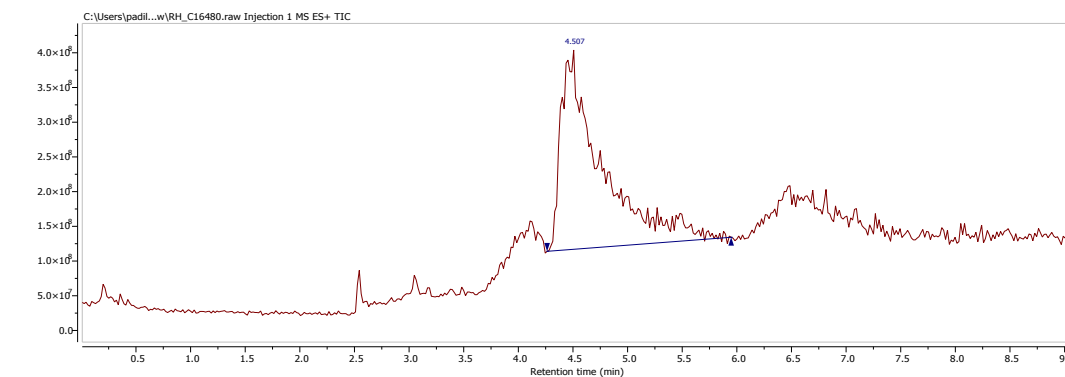
C16-1



C16-1

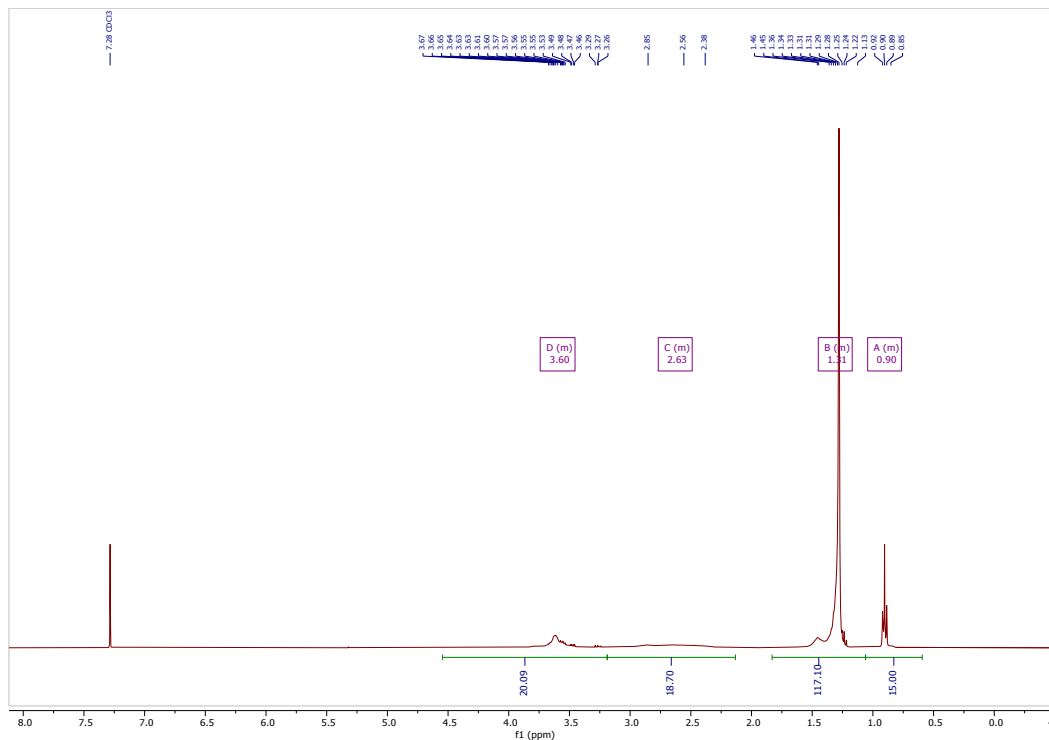
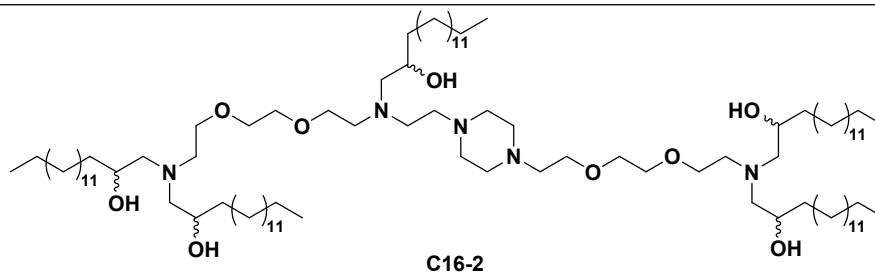


^1H NMR
(400
MHz,
 CDCl_3) δ
4.55 –
3.12 (m,
9H), 3.01
– 2.05 (m,
23H), 1.79
– 1.05 (m,
117H),
0.90 (t,
15H).

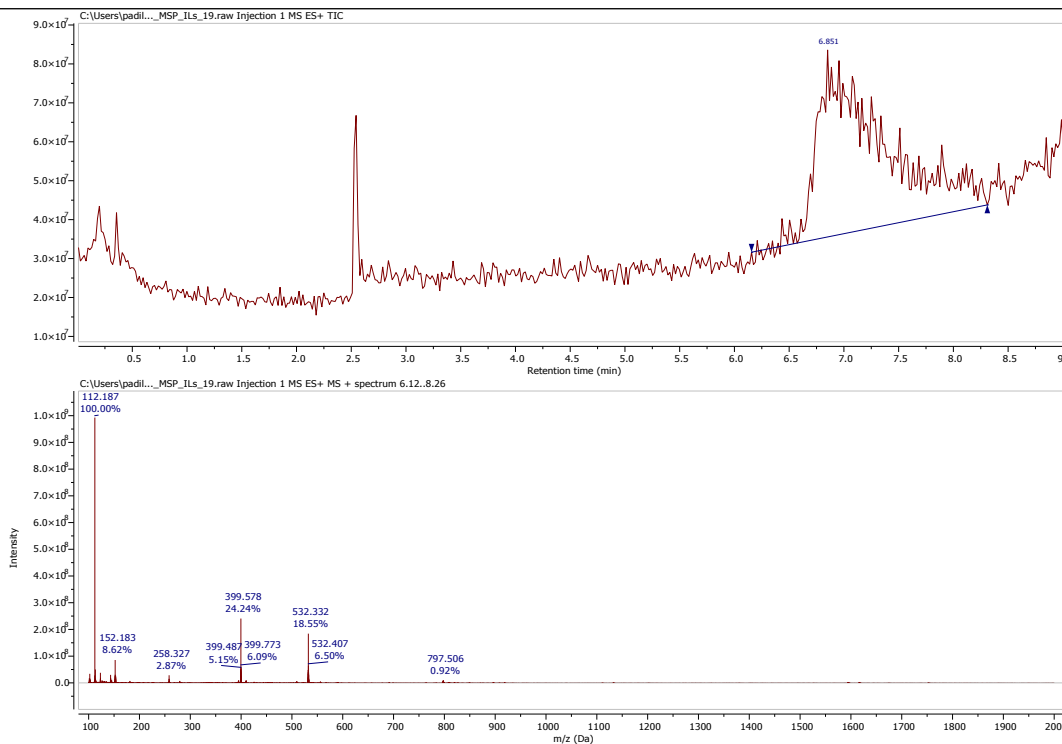


MS (ESI):
calculated
1697.91;
found
849.80
(m/2).

C16-2

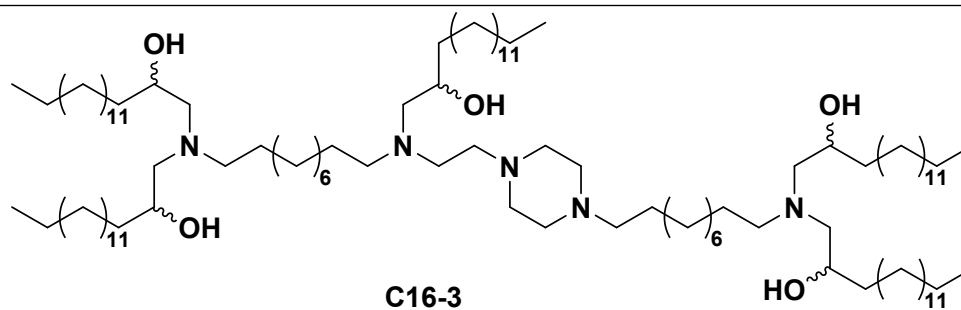


¹H NMR
(400
MHz,
CDCl₃) δ
4.53 –
3.17 (m,
20H), 3.09
– 2.12 (m,
19H), 1.71
– 1.04 (m,
117H),
1.08 –
0.65 (m,
15H).

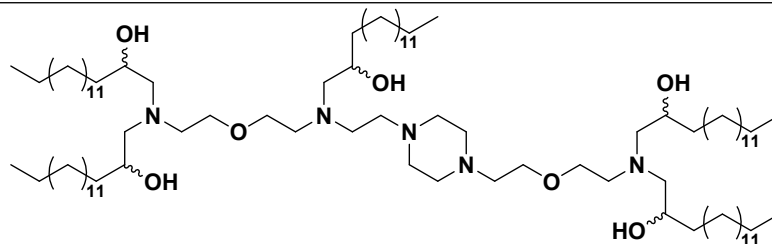


MS (ESI):
 calculated
 1593.66 ;
 found
 797.51
 (m/2).

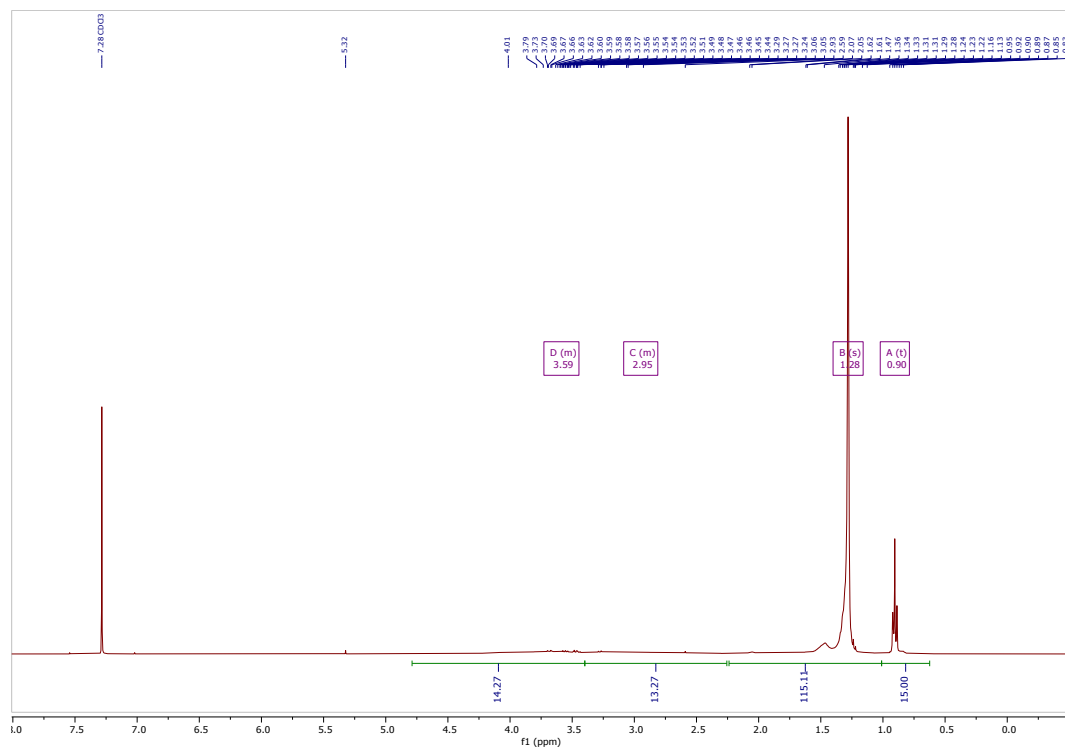
C16-3



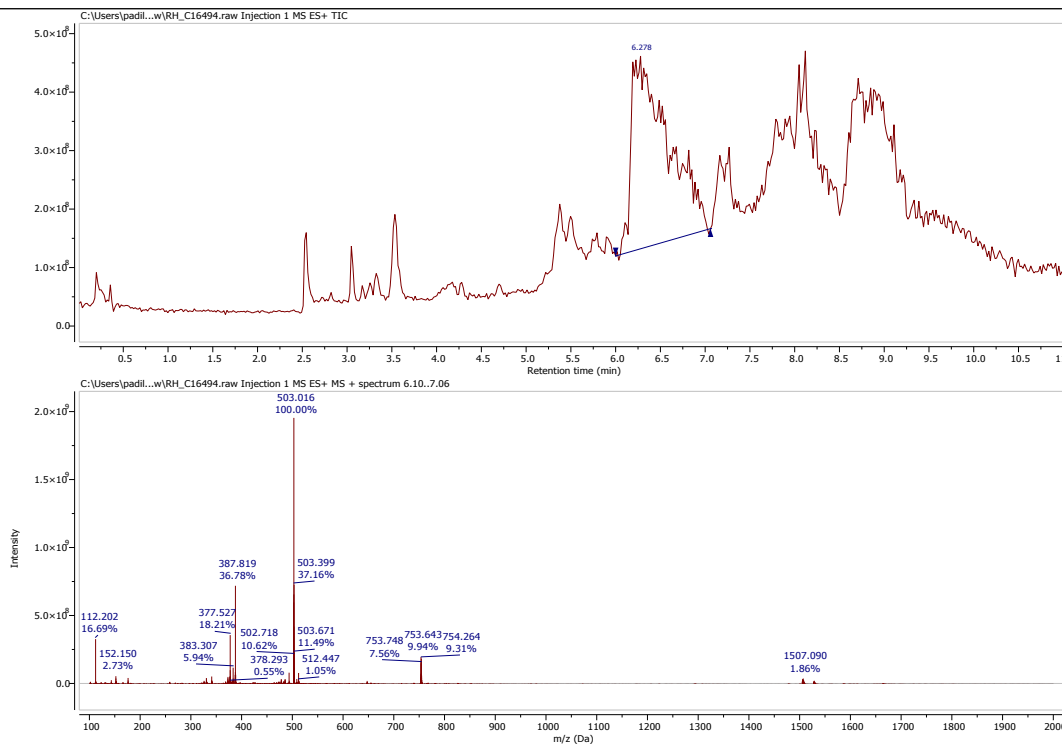
C16-4



C16-4

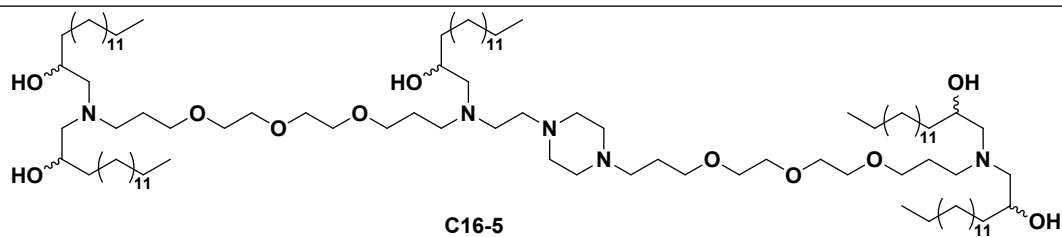


¹H NMR
(400
MHz,
CDCl₃) δ
4.54 –
3.42 (m,
14H), 3.36
– 2.27 (m,
13H), 1.28
(s, 115H),
0.90 (t,
15H).

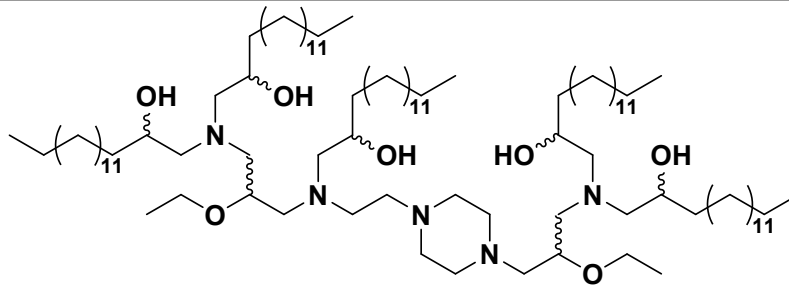


MS (ESI):
 calculated
 1505.55;
 found
 1507.09.

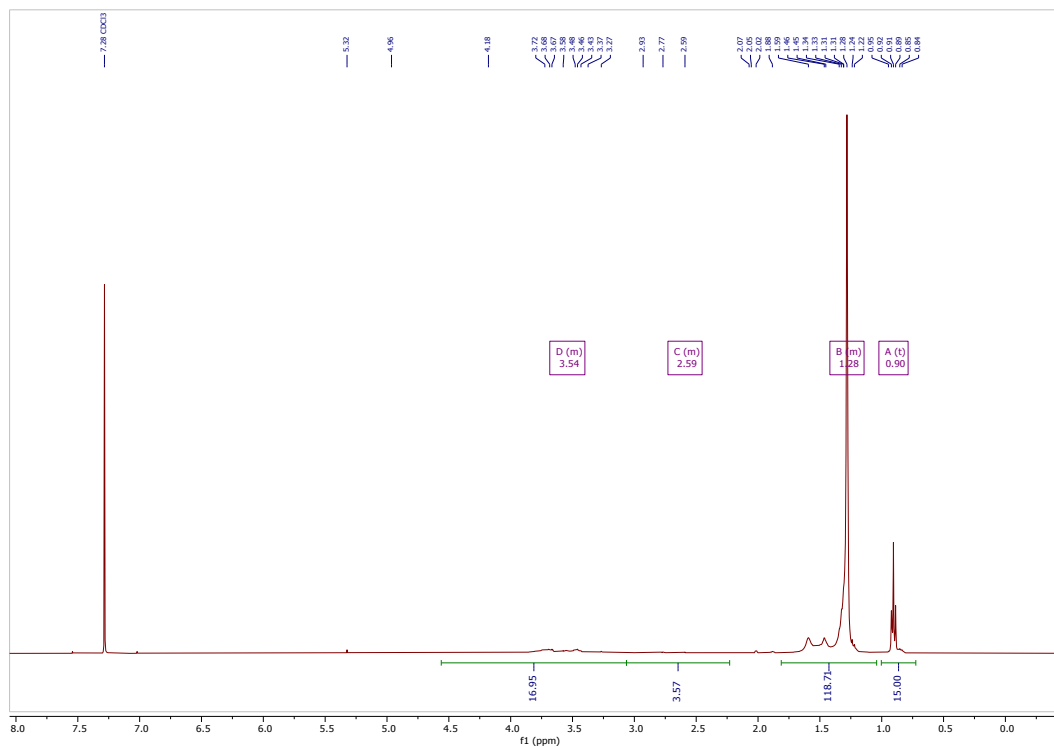
C16-5



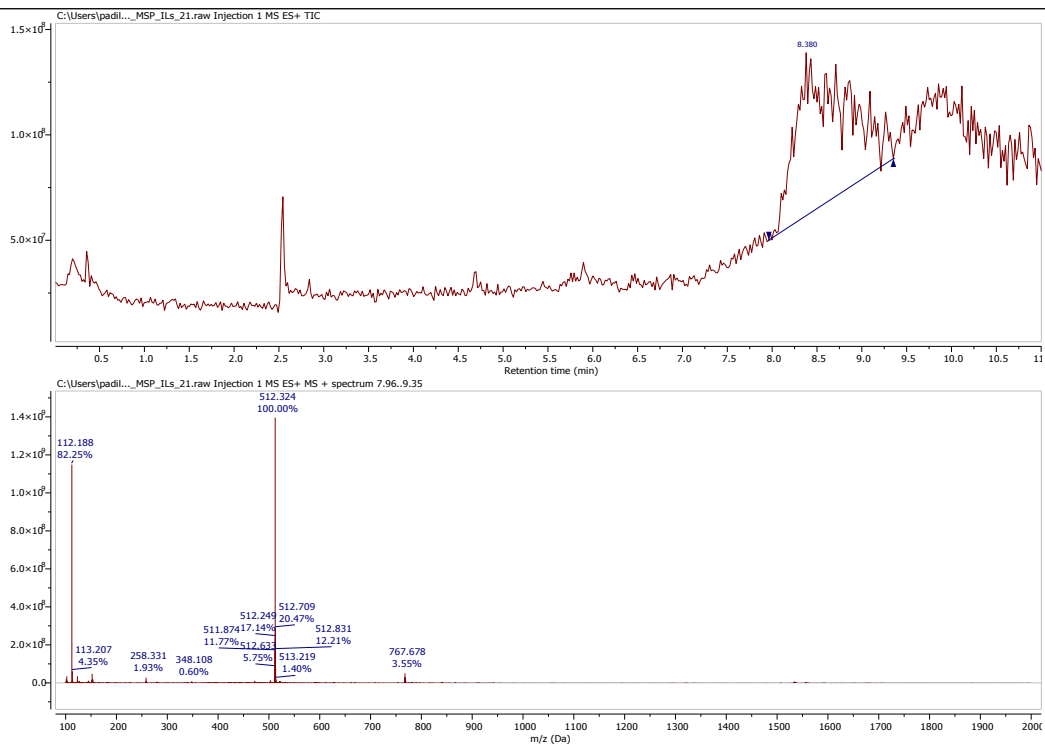
C16-6



C16-6

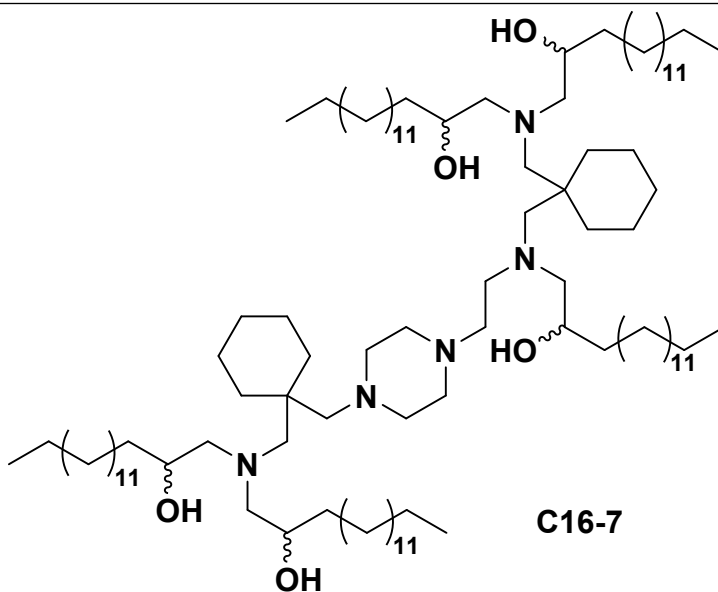


¹H NMR
(400
MHz,
CDCl₃) δ
4.55 –
3.07 (m,
17H), 3.07
– 2.15 (m,
4H), 1.73
– 1.07 (m,
119H),
0.90 (t, *J*
= 6.8 Hz,
15H).



MS (ESI):
 calculated
 1533.61;
 found
 767.68
 (m/2).

C16-7



C16-7

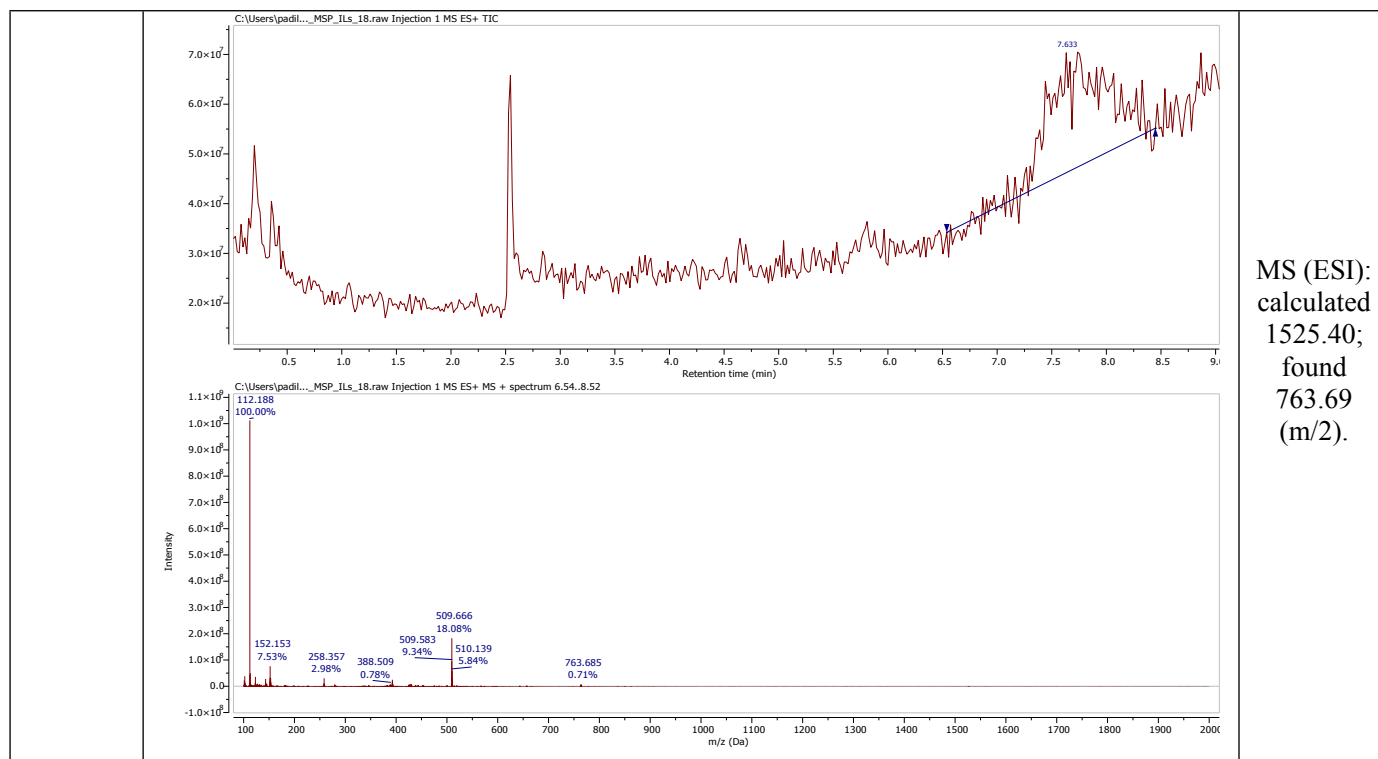


Table S3. Abbreviations and nomenclature used throughout the manuscript.

DARPin	designed ankyrin repeat protein
LNP	lipid nanoparticle
DOE	design of experiments
HTVI	hydrodynamic tail vein injection
IVIS	<i>in vivo</i> imaging system
AFP	alpha-fetoprotein
LR	Lactated Ringer's solution
DSPC	1,2-distearoyl-sn-glycero-3-phosphocholine
DOPE	1,2-dioleoyl-sn-glycero-3-phosphoethanolamine
DOPC	1,2-dioleoyl-sn-glycero-3-phosphocholine
DOTAP	1,2-dioleoyl-3-trimethylammonium-propane
PEG	polyethylene glycol
TAMRA	carboxytetramethyl rhodamine
K27	pan-RAS binding DARPin
K27n3	non-functional control DARPin

D30	anionic polypeptide sequence
S1-10	large unit of GFP, expressed by reporter cells
S11	small unit of GFP, fused to K27
LgBiT	large unit of NanoLuc, expressed by reporter cells
HiBiT	small unit of NanoLuc, fused to K27